수의학석사학위논문

고포도당에 의한 신경세포 자멸사에 멜라토닌 매개 MT_2/Akt/NF-kB 신호전달 경로를 통한 PINK1 발현이 미치는 영향

Implication of PINK1 expression via melatonin-mediated MT_2/Akt/NF-κB signaling pathway on high glucose-induced neuronal cell apoptosis

2017년 8월

서울대학교 대학원

수의학과 수의생명과학 전공

사이캄 언파잔

ABSTRACT

Implication of PINK1 expression via melatonin-mediated MT_2/Akt/NF-κB signaling pathway on high glucose-induced neuronal cell apoptosis

Xaykham ONPHACHANH
Major in Veterinary Biomedical Science
Department of Veterinary Medicine
The Graduate School
Seoul National University

Hyperglycemia is a representative hallmark and risk factor for diabetes mellitus (DM) and is closely linked to DM-associated neuronal cell death. Previous investigators reported on a genome-wide association study and showed relationships between DM and melatonin receptor (MT), highlighting the role of MT signaling by

assessing melatonin in DM. However, the role of MT signaling in DM pathogenesis is unclear. Therefore, this present study investigated the role of mitophagy regulators in high glucose-induced neuronal cell death and the effect of melatonin against high glucose-induced mitophagy regulators in neuronal cells. In the present study results, High glucose significantly increased PINK1 and LC-3B expressions, as well it decreased COX4 expression and Mitotracker™ fluorescence intensity. Silencing of PINK1 stimulated mitochondrial ROS accumulation and mitochondrial membrane potential impairment, and increased expression of cleaved caspase and the number of annexin V-positive cells. Furthermore, melatonin-increased PINK1 expression in neuronal cells was reversed by ROS scavenger pretreatment. In addition, high glucose-stimulated melatonin receptor 1B (*MTNR1B*) mRNA expression was reversed by ROS scavenger pretreatment. Up-regulation of PINK1 expression in neuronal cells is suppressed by pretreatment with MT_2 receptor-specific inhibitor. Melatonin stimulated Akt phosphorylation, which was followed by NF-κB phosphorylation and nuclear translocation. Pretreatment with NF-κB inhibitor suppressed melatonin-induced PINK1 expression. Silencing of PINK1 expression abolished melatonin-regulated mitochondrial

ROS production, cleaved caspases expressions, and increased the number of annexin V-positive cells. In conclusion, the present study have demonstrated the melatonin stimulates PINK1 expression via an MT_2/Akt/NF-κB pathway, and such stimulation is important for the prevention of neuronal cell apoptosis under high glucose conditions.

Keywords: Diabetes mellitus, Glucose, Melatonin, Mitophagy, PINK1, Neuronal cell apoptosis

Student Number: 2015-22386

CONTENTS

LIST OF FIGURES

LIST OF TABLES

ABBREVIATIONS

DM	Diabetes mellitus
PINK1	PTEN-induced putative kinase 1
BNIP3	Bcl2/adenovirus E1B 19 kDa protein-interacting protein 3
ROS	Reactive oxygen species
MT	Melatonin receptor
T2DM	Type 2 diabetes mellitus
TMRE	Tetramethylrhodamine, ethyl ester
NAC	N-acetyl cysteine
NRF	Nuclear factor (erythroid-derived 2)-like 2
HRP	Horse radish peroxidase
siRNA	Small interfering RNAs
FBS	Fetal bovine serum
DMEM	Dulbeco's essential medium
PBS	Phosphate buffered solution
BCA	Bicinchoninic acid
SDS-PAGE	Sodium dodecyl sulfate-polyacrylamide gel
DCFDA	CM-H_2DCF-DA

PCR	Polymerase chain reaction
FITC	Fluorescein isothiocyanate
PI	Propidium iodide
NF-κB	Nuclear factor kappa-light-chain-enhancer of activated B cells
LC-3B	Microtubule-associated proteins 1A/1B light chain 3B
ROD	Relative optical density
COX4	Cytochrome c oxidase subunit 4

INTRODUCTION

Hyperglycemia is a major hallmark of diabetes mellitus (DM), which leads to diabetic complications including neuronal degeneration (Moussavi et al., 2007) (Fan et al., 2016) (Kumar et al., 2017). Many reports have shown increases in hippocampal and cortical neuron apoptosis and reductions in hippocampal neuronal volume in diabetic patients (den Heijer et al., 2003) (Saravia et al., 2006). These results suggest that neuronal cell apoptosis is a representative phenomenon indicating the pathological progress of DM-associated neurodegeneration, thus suggesting the need for development of a strategy for suppressing neuronal apoptosis in DM patients with hyperglycemia. In addition, previous researchers have reported that oxidative stress induced by hyperglycemia is an essential pathogenic factor contributing to several DM-associated complications (Sima, 2010; Vikram et al., 2014). Recently, several researchers reported a relationship between mitophagy-regulated oxidative stress and the pathogenesis of diabetic heart and diabetic neuropathy, indicating that the interest of researchers in the protective action of mitophagy in DM

patients has increased (Huang et al., 2016; Tang et al., 2015). It has been shown that PTEN-induced putative kinase 1 (PINK1), Bcl2/adenovirus E1B 19 kDa protein-interacting protein 3 (BNIP3), and NIX are major mitophagy regulators that can trigger mitophagy under oxidative and metabolic stress conditions (Frank et al., 2012; Liu et al., 2014; Melser et al., 2013). Although there have been many investigations into mitophagy regulators under oxidative stress conditions, the role of ROS in expression and activation of mitophagy regulators is dependent on cell type and the physiological environment (Bellot et al., 2009; Gandhi et al., 2009; Liu et al., 2014). A previous study reported that impairment of PINK1-dependent mitophagy is closely related to diabetes susceptibility and proposed that PINK1 is a key factor in DM pathogenesis (Soleimanpour et al., 2014). Moreover, some reports have suggested that regulation of mitophagy is a promising therapeutic strategy for protection against both severe oxidative stress in DM and DM-associated complications (Hoshino et al., 2014; Lee et al., 2016b; Lo et al., 2010). However, there are few reports showing the effect of hyperglycemia on mitophagy regulation in neuronal cells. Therefore, the present study investigated details of the signaling pathway regulating mitophagy of neuronal cell under high

glucose conditions in order to provide important insights into the prevention of neuronal cell death.

Melatonin (N-acetyl-5-methoxytyptamine) is produced and secreted from non-neural tissue as well as the pineal gland, which is involved in cellular physiological functions (Manchester et al., 2015; Reiter et al., 2016). Melatonin signaling is induced by two types of G-protein-coupled receptors; melatonin receptor 1A (MT_1, encoded by MTNR1A) and melatonin receptor 1B (MT_2, encoded by MTNR1B) (Jockers et al., 2008). Results of genome-wide association studies have shown a relationship between variation of MT_2 (MTNR1B) in pancreatic islet cells and Type 2 DM (T2DM) occurrence, highlighting the role of MT_2 in T2DM pathogenesis (Lyssenko et al., 2009; Staiger et al., 2008). Previous data suggested that decreased melatonin signaling through deleterious MT_2 receptor activity increases type 2 diabetes risk (Bonnefond and Froguel, 2017). These results were line with various studies, which showed that high melatonin levels lead to decreased risk of diabetes (Costes et al., 2015; McMullan et al., 2013). However, increased melatonin signaling is a risk factor for T2DM (Tuomi et al., 2016). Thus far, the mechanisms underlying these discrepancies actions remain elusive. Regardless, it has been

determined that melatonin's antioxidative effect is induced through various mechanisms that regulate its direct and indirect oxidative stress suppressive actions (Manchester et al., 2015; Reiter et al., 2016). In addition, the melatonin-activated intracellular antioxidative system is effective in the prevention of neuronal cell apoptosis in neurodegenerative disease models (Antolin et al., 2002; Chen and Chuang, 1999; Mattson, 2000), Several studies have focused on the role of melatonin in mitophagy regulation (Coto-Montes et al., 2012; Kang et al., 2016; Wang et al., 2015a). In particular, recent reports on the effect of melatonin on PINK1 expression have provided new insights into melatonin application and mitophagy regulation (Diaz-Casado et al., 2016; Kang et al., 2016). However, which mitophagy regulators contribute to the mitophagy-induced antioxidative effect of melatonin in DM patients has been incompletely elucidated. In addition, studies into the melatonin-signaling mechanism in mitophagy regulation are required to describe fully melatonin's protective role.

The SK-N-MC and SH-SY5Y neuroblastoma cell lines and mouse hippocampal neurons have been widely used for investigating the pathogenesis of neuronal diseases related to hyperglycemia and DM (Lee et al., 2016a; Li et al., 2014; Wang et al., 2015b) (Suzuki et al.,

2012). Moreover, use of the neuronal cell lines has advantages in studies into the identification of molecular mechanism due to their high homogeneity and reproducibility. And, Identifying and describing in detail the mechanism involved in the signaling pathway controlling mitophagy regulators under high glucose conditions and elucidating the actions of melatonin in neuronal cell models are important for the development of an effective therapeutic strategy for hyperglycemia-induced neuronal cell death. Therefore, this present study investigated the role of mitophagy regulators mediated by high glucose in neuronal cell death and the regulatory mechanism of melatonin against mitophagy regulators in neuronal cells under high glucose conditions.

MATERIALS AND METHODS

1. Materials

Human neuroblastoma cells of the SK-N-MC and SH-SY5Y cell lines were kindly provided by the Korean Cell Line Bank (Seoul, Korea). Fetal bovine serum (FBS) was purchased from Hyclone (Logan, UT, USA), while BNIP3, NIX, Mitofusin-2 (Mfn2), p-Akt(Thr308), p–Akt (Ser473), Akt, p-NFκB (Ser536), nuclear factor kappa-light-chain-enhancer of activated B cells (NFκB), p-ERK (Tyr204), ERK, PKC, MT_2, lamin A/C, β-actin, β-tubulin, MT_1, and caspase-9 antibodies were purchased from Santa Cruz Biotechnology (Dallas, TX, USA). PINK1, microtubule-associated proteins 1A/1B light chain 3B (LC-3B), and MT_2 antibodies were purchased from Novus Biologicals (USA). p-pan PKC (βII Ser660) and caspase-3 antibodies were purchased from Cell Signaling Technology (Beverly, MA, USA). Cytochrome c oxidase subunit 4 (COX4) antibody was purchased from Abcam (Cambridge, MA, USA). Ubiquitin antibody was purchased from AbFrontier (Seoul, Korea). Horseradish peroxidase (HRP)-conjugated rabbit anti-mouse

and goat anti-rabbit secondary antibodies were purchased from Thermo Fisher (Waltham, MA, USA), Melatonin (Mel, 5-methoxy-N-acetyltryptamine) was obtained from Sigma Chemical (St. Louis, MO, USA), while D-glucose, L-glucose, N-acetyl cysteine (NAC), LY294002, SN50, 4-P-PDOT, and propidium iodide (PI) were obtained from Sigma-Aldrich (St. Louis, MO, USA), small interfering RNAs (siRNAs) for PINK1, and non-targeting (NT) siRNAs were purchased from Dharmacon (Lafayette, CO, USA). All reagents used in this study were high-quality commercial preparations.

2. Cell culture

The SK-N-MC and SH-SY5Y cells were cultured in 5×10^5 cells/60 mm dish in 3 mL high glucose Dulbecco's essential medium (DMEM; Gibco, Grand Island, NY, USA) including 10% FBS, 1% antibiotic (penicillin, streptomycin, and fungizone) high glucose Dulbecco's essential medium (DMEM; Gibco). The cells were incubated at 37°C with 5% CO_2 for 72 h, which was followed by washing with PBS. The growth medium was then changed to serum-free high glucose DMEM for an additional 24 h. After starvation, cells were plated with high glucose DMEM and reagents.

3. Primary culture of mouse hippocampal neurons

Mouse hippocampus was isolated from brain of 17-day mouse embryo with 0.05% trypsin solution. After isolation, dissociated cells were counted by using a hemocytometer and 2×10^5 dissociated cells were plated on poly-D-lysine coated 35 mm dishes with neurobasal plating medium [neurobasal medium (Gibco) containing B27 supplement (1 mL/50 mL), 25 μM glutamate (Sigma-Aldrich), 0.5 mM, glutamine (Sigma-Aldrich), 10% horse serum (Gibco), and 1 mM HEPES (Sigma-Aldrich)]. Cells were incubated at 37°C with 5 % CO_2 for 24 h. After incubation, neuronal cells replaced with same volume of neurobasal feeding medium [neurobasal medium containing B27 supplement (1 mL/50 mL), 0.5 mM, glutamine, 10% horse serum, 1 mM HEPES) and 5 μM of cytosine arabinoside (AraC; Sigma-Aldrich)]. After incubation of 24 h, the medium was changed to neurobasal feeding medium without AraC. Neuronal cells were then cultured for 12 d. All primary hippocampal culture protocols followed the National Institutes of Health Guidelines for the Humane Treatment of Animals. This protocol was approved by the Institutional Animal Care and Use Committee of Seoul National University (SNU-151116-1).

4. RNA isolation and reverse transcription-polymerase chain reaction

RNA samples were extracted by using a commercial RNA extraction kit (TaKaRa Biomedical, Otsu, Japan). Reverse transcription-polymerase chain reaction (RT-PCR) was performed with 1 μg of extracted RNA and a Maxime™ RT-PCR premix kit (iNtRON Biotechnology, Sungnam, Korea) to produce cDNA. RT-PCR was performed for 1 h at 45°C and 5 min at 95°C.

5. Real Time quantitative PCR

The cDNA sample was amplified with a QuantiSpeed™ SYBR kit (Life Technologies, Gaithersburg, MD, USA). The mRNA expression levels of the PINK1, BNIP3, NIX, MTNR1A, MTNR1B, and ACTB genes were determined by using a Rotor-Gene 6000 real-time thermal cycling system (Corbett Research, Mortlake, NSW, Australia) with mRNA primers and 1 μg of cDNA sample. The primer sequences of mRNAs are described in Supplementary table.1 Melting curve analysis was performed by using software provided by Rotor-Gene 6000 Series software (Life Technologies) to confirm the identity and specificity of

the real-time polymerase chain reaction (PCR) products. Gene expression level was normalized to the mRNA expression of ACTB.

Table 1. Sequences of primers used for RT-PCR and real-time PCR

Gene name	Species	Identification	Sequence (5'-3')	Size (bp)
MTNR1A	Human	Sense	TGTCGATATTTAACAACGGGTGG	108
		Antisense	CGATGCCGGTGATGTTGAA	
MTNR1B	Human	Sense	GCATGGCCTACCACCGAATC	201
		Antisense	AATAGATGCGTGGGTCGTACT	
ACTB	Human	Sense	AACCGCGAGAAGATGACC	351
		Antisense	AGCAGCCGTGGCCATCTC	

6. Small interfering RNA transfection

Prior to performing small-interfering (si) RNA transfection, cells were grown until 70% of the dish surface was covered. PINK1 (cat no. L-004030-00-0005, Dharmacon) -specific or NT (cat no. L-001206-13-20, Dharmacon) siRNAs (20 nM) were transfected into cells for 24 h along with Turbofect™ transfection reagent (Thermo Fisher)

according to the manufacturer's manual. Subsequently, cells were incubated at 37°C with 5% CO2 for 24 h. The siRNAs sequences of PINK1 and NT are described in Table 2.

Table 2. Sequences of siRNAs used for gene silencing

Target gene	Sequences 5'-3'	Manufacturer
PINK1	GCAAAUGUGCUUCAUCUAA GCUUUCGGCUGGAGGAGUA GGACGCUGUUCCUCGUUAU GAGACCAUCUGCCCGAGUA	Dharmacon
Non-targeting	UAGCGACUAAACACAUCAA UUGAUGUGUUUAGUCGCUA	Dharmacon

7. Trypan blue exclusion cell viability assay

Fluo 3-AM(2 μM) was used to detect the intracellular calcium levels. The cells were plated on confocal dishes and were washed with a PBS once. The cells were then incubated in PBS containing 3 μM Fluo 3-AM with 5% CO2 at 37°C for 40 minutes. The cells were imaged using laser confocal microscopy (X400) (Fluo View 300) with an excitation wavelength of 488 nm and an emission wavelength of 515 nm.

Ionomycin was applied as a positive control. Analysis of intracellular calcium levels processed at a single cell level are expressed as the relative fluorescence intensity (RFI).

8. Nuclear fraction preparation

Harvested cells were lysed in nuclear fraction lysis buffer [1 mM dithiothreitol, 0.1 mM PMSF ,8.1 mM Na2HPO4, 137 mM NaCl, 1.5 mM KH2PO4, 2.7 mM KCl, 2.5 mM EDTA, and 10 mg/mL leupeptin (pH 7.5)] by pipetting and incubated for 10 min on ice. Cell lysates were centrifugated at 3000 r/min at 4℃ for 5 min, and the supernatant was collected as a non-nuclear fraction. The residual pellet was lysed with RIPA lysis buffer on ice for 25 min, and subsequently centrifugated at 15,000 r/min at 4℃ for 30 min. The supernatant, as the nuclear fraction, was collected.

9. Western blot analysis

Cells were harvested, washed twice with cold PBS, collected by using a cell scraper, and lysed with RIPA buffer (Thermo Fisher) and

a proteinase and phosphatase inhibitor (Thermo Fisher) for 30 min on ice. The lysates were then cleared via centrifugation (15,000 r/min at 4°C for 30 min), and the supernatant was collected. The protein concentration was determined by using a bicinchoninic acid (BCA) assay kit (Thermo Fisher). Equal amounts of protein (10 μg) were loaded in 8%–15% sodium dodecyl sulfate-polyacrylamide gel (SDS-PAGE) for electrophoresis. Proteins were transferred to a polyvinylidene fluoride (PVDF) membrane, and the membrane washed with TBST solution [150 mM NaCl, 10 mM Tris-HCl (pH 7.6), and 0.1% Tween-20]. The membrane was blocked with 5% skim milk (Gibco) and 5% bovine serum albumin (Sigma-Aldrich) in TBST solution for 1 h; subsequently, the membrane was washed with TBST and incubated with the appropriate primary antibody (1:1000) overnight at 4°C. The membrane was then washed and incubated with horseradish peroxidase (HRP)-conjugated secondary antibody (1:10,000 dilution) for 4 h at 4°C. The western blot bands were visualized by using an enhanced chemiluminescence solution (Bio-Rad, Hercules, CA, USA).

10. Preparation of co-immunoprecipitation sample

Co-immunoprecipitation was performed by using a commercial kit

(Thermo Fisher) according to supplier's manual. Harvested cells were lysed with IP lysis buffer and proteinase inhibitor cocktail (Thermo Fisher). Lysate samples were immunoprecipitated by Mfn2-conjugated resin. Mfn2-interacted protein was acquired by incubation in elution buffer. Sample buffer was added to eluted sample, and boiled at 100°C for 5 min.

11. Measurements of intracellular reactive oxygen species levels

Intracellular ROS level determination was performed by using CM-H2DCF-DA staining (DCF-DA, Life Technologies). Cells were washed twice with phosphate buffered solution (PBS) and incubated with 0.05% trypsin for 5 min. Dissociated cells (5 × 105) were centrifugated at 4000 r/min for 5 min and then incubated in the dark with 10 μM DCF-DA in PBS for 30 min at 37°C. Cells were then washed with PBS and 100 μL of cell suspension was loaded in a 96-well black plate, and staining results measured by luminometer (Victor3, Perkin-Elmer, Waltham, MA, USA).

12. Annexin V/PI fluorescence-activated cell sorter analysis

Annexin V and PI double staining was performed by using an annexin V/PI apoptosis detection kit (BD Bioscience, Franklin Lakes, NJ, USA) according to the manufacturer's manual. After treatment, cells were detached with 0.05% trypsin. Cells were counted 1 × 105 cells, followed by centrifugation at 4,000 r/min for 5 min. Cells were then resuspended in the binding buffer supplied with the apoptosis detection kit, and immunostained with 5 μL of fluorescein isothiocyanate (FITC) conjugated Annexin V and 5 μL of PI for 15 min at room temperature. Cell apoptosis was measured by using flow cytometry (Beckman Coulter, Fullerton, CA, USA). Data were analyzed by using CXP software (Beckman Coulter). Annexin V-positive with PI-positive (Q2) or PI-negative cells (Q4) and Annexin V-negative with PI-positive cells (Q1) were considered apoptotic. Annexin V-negative and PI-negative cells (Q3) were considered viable. To determine the percentage of apoptotic cells, the following formula was used: Apoptotic cells = Q1 + Q2 + Q4.

13. Immunocytochemistry

Cells were cultured in a confocal dish (Thermo Fisher). After treatment, cells were fixed with 80% acetone in PBS for 10 min at −20°C. To inhibit non-specific binding of antibodies, cells were incubated with 5% normal goat serum (Sigma-Aldrich) in PBS. Subsequently, cells were incubated with a 1:100 dilution of primary antibody for 2 h at room temperature. After washing, cells were incubated with Alexa fluor-conjugated secondary antibody and PI for 1 h at room temperature. Images were obtained by using a Fluoview 300 confocal microscope (Olympus, Tokyo, Japan). Fluorescence intensity was analyzed by using ImageJ software (developed by Wayne Rasband, National Institutes of Health, Bethesda, MD, USA; http://rsb.info.nih.go.kr/ij/).

14. Measurement of mitochondrial ROS generation

To evaluate the generation of mitochondrial ROS, MitoSOX™ mitochondrial superoxide indicator (Thermo Fisher) was used. Cells were washed with PBS and then incubated with 10 μM MitoSOX™

solution in PBS at 37°C for 15 min. Cells were again washed with PBS and incubated with 0.05% trypsin for 5 min. Cells were then washed twice with PBS, followed by suspending the cells in 500 μL PBS. MitoSOX™-positive cells were detected by using flow cytometry (Beckman Coulter). Cells that had similar side scatter and forward scatter levels were analyzed by using Flowing Software (developed by Perttu Terho, Turku, Finland).

15. Measurement of mitochondrial membrane potential

To measure mitochondrial membrane potential, TMRE (Sigma-Aldrich) was used. After treatment, cells were washed with PBS and incubated with 200 nM of TMRE solution in PBS at 37°C for 30 min. Cells were then washed with PBS and detached by using 0.05% trypsin solution. Detached cells were washed twice with PBS and suspended with 500 μL of PBS. TMRE-positive cells were detected by using flow cytometry (Beckman Coulter). Cells that had similar side scatter and forward scatter levels were analyzed by using Flowing Software (developed by Perttu Terho, Turku, Finland).

16. Statistical analysis

All quantitative data are presented as a mean value ± standard error of mean (S.E.M). Comparisons of treatment means with that of control groups were conducted by using Student's t-test for two group analysis. Differential among experimental groups were analyzed by using ANOVA. A p-value < 0.05 was considered statistically significant.

RESULTS

1. Effect of high glucose on PINK1-mediated mitophagy in neuronal cells

To determine the effect of high glucose on mitophagy regulator expression in SK-N-MC cells. As shown in Figure 1A, PINK1 mRNA expression was significantly increased at 25 and 50 mM D-glucose, but BNIP3 and NIX mRNA expressions were not affected by D-glucose treatment. In addition, PINK1 increased and COX4 expressions decreased in a D-glucose dose-dependent manner (Fig. 1B). Moreover, 24 h and 48 h treatment with high D-glucose increased PINK1 expression (Fig. 1C), whereas 24 h of L-glucose treatment did not affect PINK1 expression in SK-N-MC and SHSY-5Y cells or in mouse hippocampal neurons (Figs. 2A–2C). To assess the effect of high glucose on mitophagy, this present study determined the mitochondrial volume in SK-N-MC cells by using mitochondrial specific fluorescent dye Mitotracker™ and mitochondrial marker COX4. Immunofluorescence results showed that the fluorescence intensities

of Mitotracker™ in SK-N-MC cells with high glucose treatment for 24 h and 48 h were reduced to 71.2% and 37.0% of the control level respectively (Fig. 3A). The fluorescence intensities of COX4 following 24 h and 48 h of high glucose decreased to 68.8% and 42.4 %, respectively, of the control level (Fig. 3B). In addition, high glucose treatment increased co-localization of COX4 with PINK1 or microtubule-associated proteins 1A/1B light chain 3B (LC-3B) (Figs. 3C and 3D). Present study pretreated NH4Cl as an autophagy inhibitor prior to D-glucose incubation to confirm the effect of D-glucose on mitophagy. the result showed NH4Cl pretreatment recovered decreased COX4 expression by D-glucose (Fig. 4). These results indicate that high glucose conditions trigger mitophagy, and mitophagy is dependent on the PINK1 pathway in neuronal cells.

A

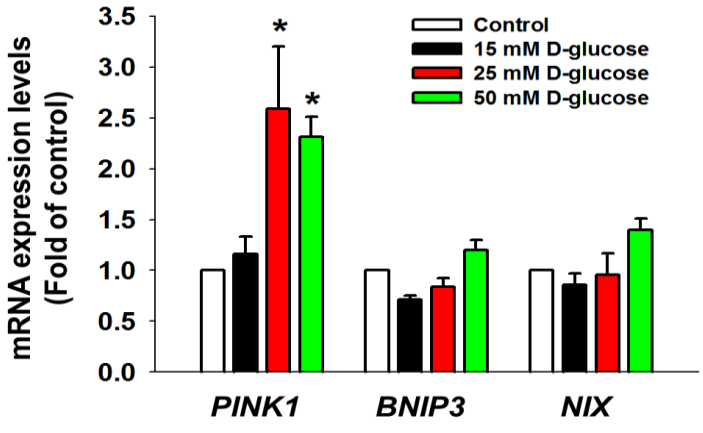
mRNA expression levels
(Fold of control)
3.5
3.0
2.5
2.0
1.5
1.0
0.5
0.0
Control
15 mM D-glucose
25 mM D-glucose
50 mM D-glucose
*
*
PINK1
BNIP3
NIX

B

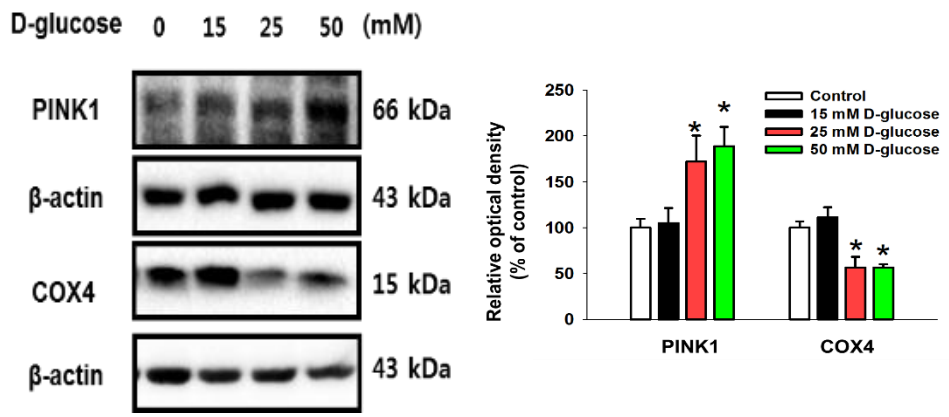
D-glucose 0 15 25 50 (mM)
PINK1
66 kDa
β-actin
43 kDa
COX4
15 kDa
β-actin
43 kDa
Relative optical density
(% of control)
250
200
150
100
50
0
Control
15 mM D-glucose
25 mM D-glucose
50 mM D-glucose
*
*
*
*
PINK1
COX4

C

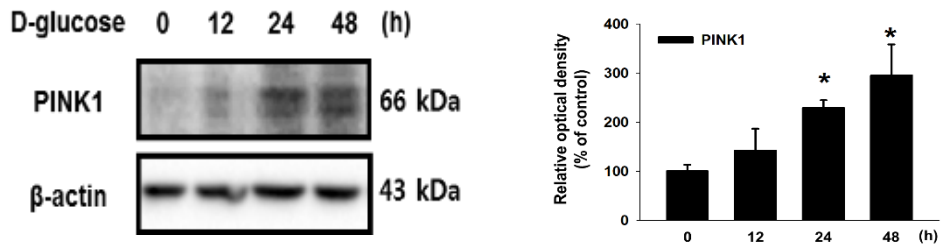
D-glucose 0 12 24 48 (h)
PINK1
66 kDa
β-actin
43 kDa
Relative optical density
(% of control)
400
300
200
100
0
PINK1
*
*
0
12
24
48
(h)

Figure 1. Effect of high glucose on PINK1 expression in neuronal cells. (A) SK-N-MCs were incubated with various concentrations of D-glucose (5–50 mM) for 24 h. The mRNA expressions of PINK1, BNIP3, NIX and ACTB were measured by quantitative real-time PCR (qPCR). mRNA expression levels were normalized by ACTB mRNA expression level. Data are presented as a mean ± S.E.M. n = 5. (B) The protein expressions of PINK1, COX4 and β-actin were assessed by western blot. Relative optical density (ROD) of PINK1 and COX4 were normalized by β-actin. ROD data are presented as a mean ± S.E.M. n = 4. (C) SK-N-MCs were incubated with various durations of 25 mM of D-glucose (0 - 48 h). The protein expressions of PINK1 and β-actin were detected by western blot. ROD data of PINK1 was normalized by β-actin. Quantitative ROD data are presented as a mean ± S.E.M. n = 4. Each blot images are representative. *$p < 0.05$ versus control.

A

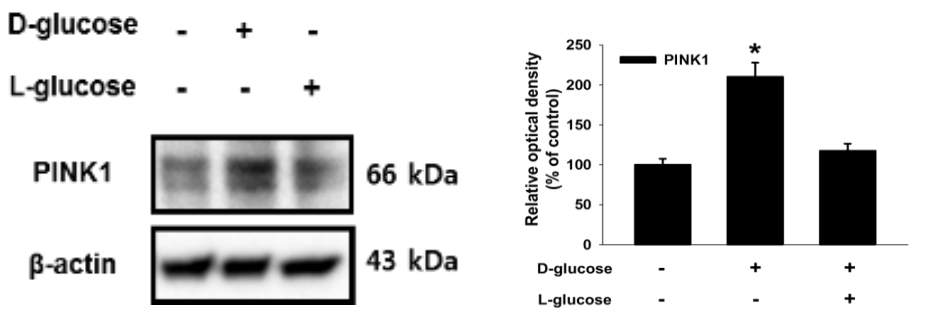
D-glucose - + -
L-glucose - - +
PINK1
66 kDa
β-actin
43 kDa
PINK1
Relative optical density (% of control)
250
200
150
100
50
0
*
D-glucose - + +
L-glucose - - +

B

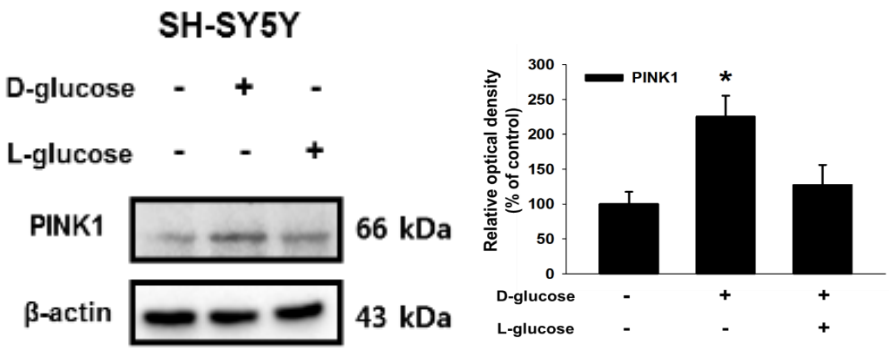
SH-SY5Y
D-glucose - + -
L-glucose - - +
PINK1
66 kDa
β-actin
43 kDa
PINK1
Relative optical density (% of control)
300
250
200
150
100
50
0
*
D-glucose - + +
L-glucose - - +

C

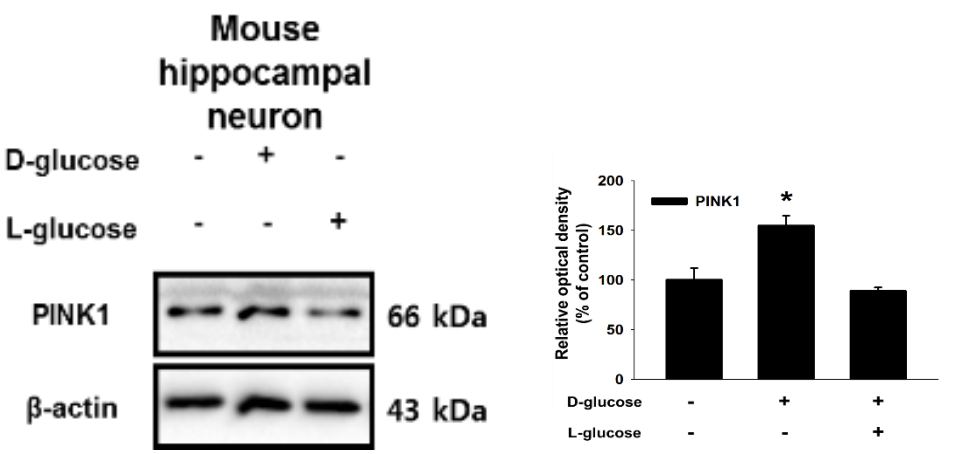
Mouse hippocampal neuron
D-glucose - + -
L-glucose - - +
PINK1
66 kDa
β-actin
43 kDa
PINK1
Relative optical density (% of control)
200
150
100
50
0
*
D-glucose - + +
L-glucose - - +

Figure 2 Effect of high glucose and Low glucose on PINK1 expression in neuronal cell in neuronal cells. (A-C) SK-N-MCs, SHSY-5Ys and mouse primary hippocampal neurons were incubated with 25 mM of D-glucose or 25 mM of L-glucose for 24 h. PINK1 and β-actin proteins were detected by western blot. ROD of PINK1 was normalized by β-actin. ROD data are presented as a mean ± S.E.M. n = 4. Each blot images are representative. *$p < 0.05$ versus control.

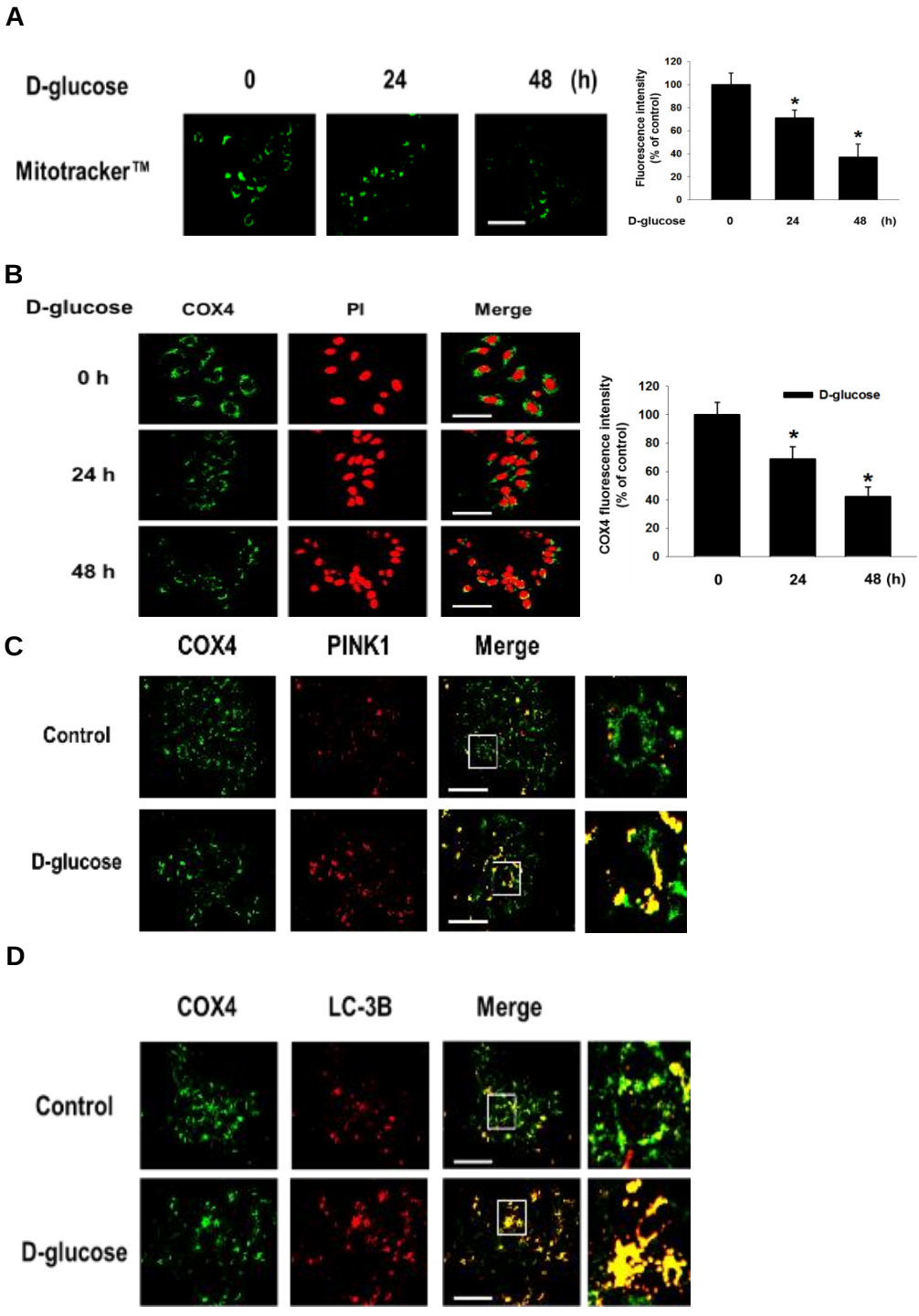
A
D-glucose
0
24
48 (h)
Mitotracker™
Fluorescence intensity (% of control)
120
100
80
60
40
20
0
D-glucose
0
24
48 (h)
B
D-glucose
COX4
PI
Merge
0 h
24 h
48 h
COX4 fluorescence intensity (% of control)
D-glucose
C
COX4
PINK1
Merge
Control
D-glucose
D
COX4
LC-3B
Merge
Control
D-glucose

Figure 3. Effect of high glucose on mitophagy in neuronal cells. (A) SK-N-MCs were exposed to various durations of 25 mM of D-glucose (0–48 h). Cells were stained with Mitotracker™. The fluorescence intensities of Mitotracker™ was presented as a mean ± S.E.M. n = 6 (magnification, ×800). All scale bars, 10 μm. (B) SK-N-MCs were incubated with 25 mM of D-glucose (0-48 h). Cells were immunostained with COX4-specific antibody and PI. The fluorescence intensities of COX4 are presented as a mean ± S.E.M. n = 6 (magnification, ×800). All scale bars, 10 μm. (C and D) SK-N-MCs were incubated with 25 mM of D-glucose for 24 h. Cells were incubated with COX4, PINK1 and LC-3B-specific antibodies for 24 h. The confocal images are representative (magnification, ×800). All scale bars, 10 μm. *$p < 0.05$ versus control.

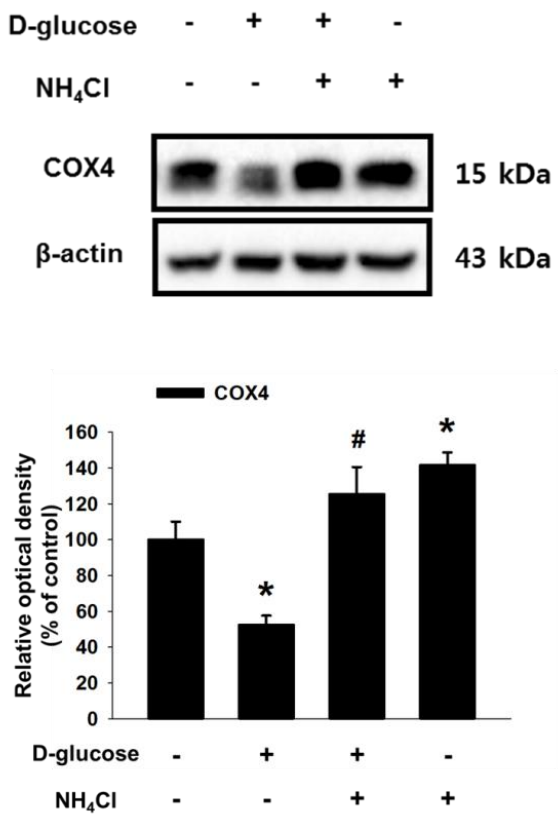

Figure. 4 Effect of NH4Cl on high glucose-reduced COX4 expression. SK-N-MCs were pretreated with NH4Cl (10 uM) for 30 min prior to D-glucose (20 mM) for 24 h. COX4 and β-actin were detected by western blot. All blot images are representative. Data are showed as a mean ± S.E.M. n = 3. *p < 0.05 versus control, #p < 0.05 versus D-glucose treatment.

2. Protective role of PINK1 in mitochondrial dysfunction and apoptosis induced by high glucose

To investigated further the role of PINK1 in high glucose-induced mitophagy. As shown in Figure 5, immunofluorescence results revealed that a high glucose- reduced COX4 fluorescence intensity was recovered by PINK1 siRNA transfection with D-glucose or vehicle. Present study observed that PINK1 siRNA transfection significantly decreased PINK1 mRNA expression levels of SK-N-MCs with D-glucose or vehicle (Fig. 6). In addition, to investigated the role of high glucose-induced PINK1 in Mfn2 ubiquitination. Present study result showed high glucose significantly increased Mfn2 ubiquitination and decreased Mfn2 expression, which were reversed by PINK1 silencing (Fig. 7). This finding presents a direct evidence for PINK1-induced mitophagy in SK-N-MCs under high glucose condition. To determine the role of high glucose in ROS accumulation, present study measured intracellular and mitochondrial-specific ROS levels in SK-N-MC cells. As shown in Figure 8, intracellular ROS level increased to 183.7% of the control level after high glucose treatment and increased further to 276.6% of the control level after PINK1 siRNA transfection with high

glucose treatment. Furthermore, ROS levels in SK-N-MCs with PINK1 siRNA transfection alone was increased to 170.2% of control. The flow cytometry results showed that silencing of PINK1with D-glucose or vehicle increased the number of MitoSOX™-positive cells and decreased the number of TMRE-positive cells. (Figs. 9A and 9B). Taken together, these results indicate that high glucose-triggered mitophagy via PINK1 induction has an essential role in the suppression of mitochondrial ROS accumulation and the maintenance of mitochondrial quality control. Next, present study investigated the role of high glucose-induced PINK1 in neuronal cell death. As shown in Figure 10A, 25 and 50 mM of D-glucose treatments stimulated cleaved caspase-3 and -9 expressions. In support of those results, trypan blue exclusion assay results showed that 25 and 50 mM D-glucose, not L-glucose, treatments reduced SK-N-MC cell viability (Fig. 10B). To determine the role of high glucose-induced PINK1 in neuronal cell death, present study transfected PINK1 siRNA into SK-N-MC cells. The western blot results showed that cleaved caspase-9 and -3 expressions in PINK1 siRNA-transfected cells with high glucose were higher than those of NT siRNA-transfected cells with high glucose (Fig. 11A). The trypan blue exclusion assay results showed decreased

cell viability in the high glucose treatment group, which was decreased further by PINK1 siRNA transfection with high glucose (Fig. 11B). Moreover, the number of annexin V-positive apoptotic cells was increased by high glucose treatment, with further significant enhancement by co-treatment of PINK1 siRNA with high glucose (Fig. 11C). Taken together, these results indicate that high glucose-induced PINK1 has a protective role in the apoptosis of SK-N-MC cells under high glucose condition.

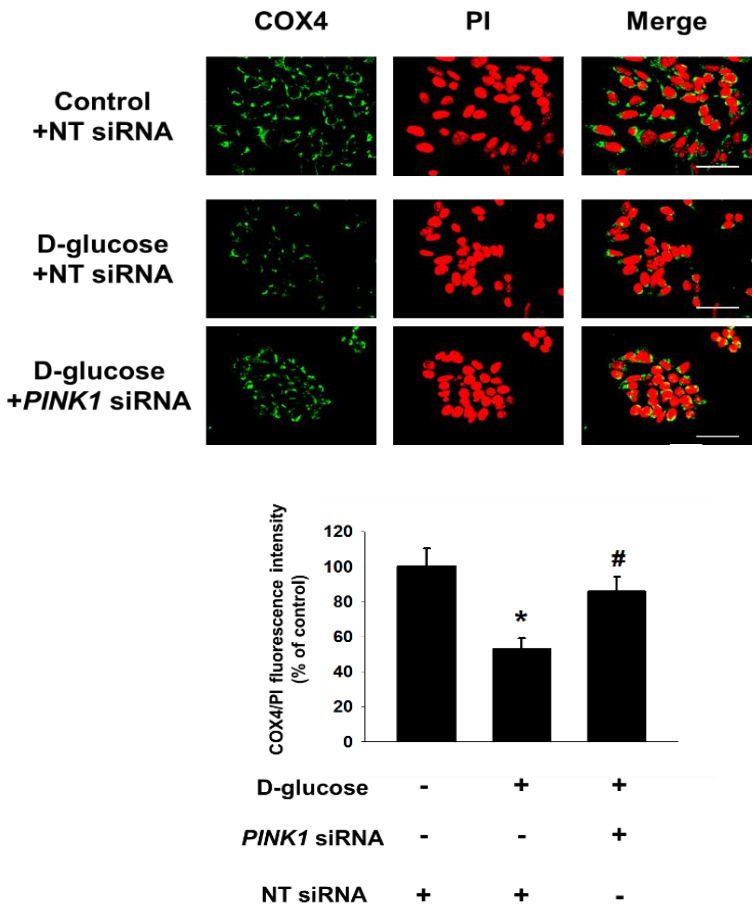

Figure 5. Role of PINK1 in the COX4 fluorescence intensity in SK-N-MCs under high glucose. PINK1 or NT siRNAs were transfected to SK-N-MCs prior to 25 mM of D-glucose treatment for 48 h. Cells were immune-stained with COX4-specific antibody and PI. The fluorescence intensities of COX4 are reported as a mean ± S.E.M. n = 6 (magnification, ×800). All scale bars, 10 μm. All confocal images are representative. Data are presented as a mean ± S.E.M. n = 6. *$p < 0.05$ versus control, #$p < 0.05$ versus D-glucose treatment.

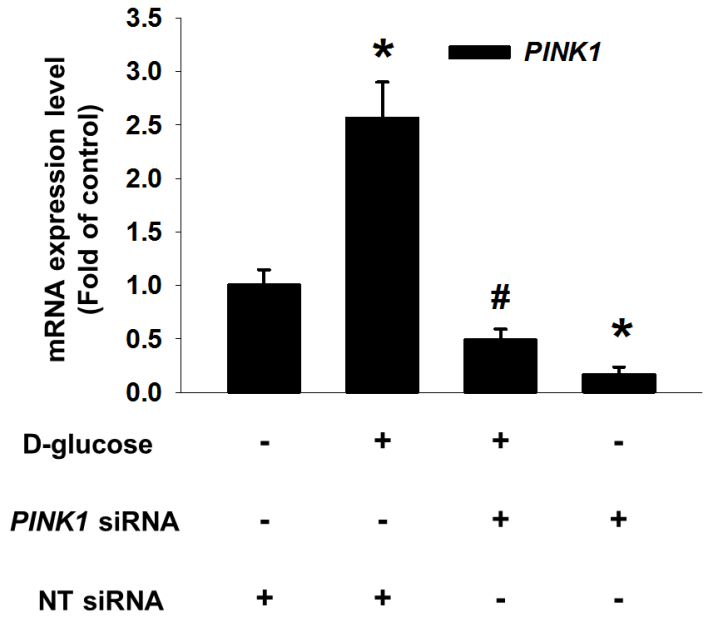

Figure 6. Effect of PINK1 siRNA on PINK1 mRNA expression in SK-N-MCs. Cells were transfected with PINK1 siRNA or NT siRNA for 24 h prior to D-glucose (25 mM) treatment for 24 h. PINK1 and ACTB mRNA expressions were analyzed by qPCR. The mRNA expression level of PINK1 was normalized by ACTB mRNA expression. Quantitative data are presented as a mean ± S.E.M. n = 5.

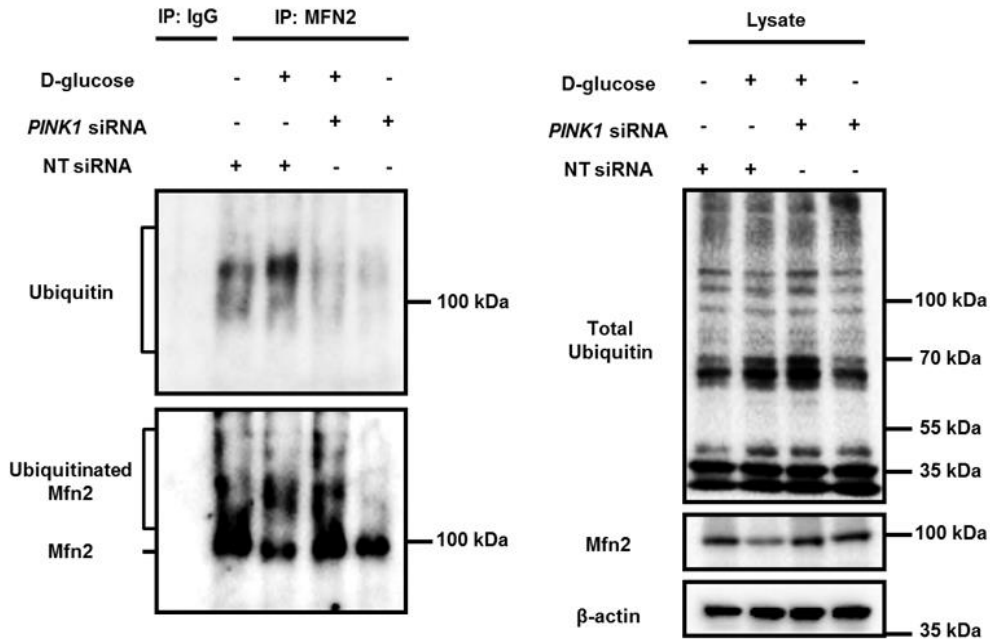
IP: IgG
IP: MFN2
D-glucose - + + -
PINK1 siRNA - - + +
NT siRNA + + - -
Ubiquitin
100 kDa
Ubiquitinated Mfn2
Mfn2
100 kDa
Lysate
D-glucose - + + -
PINK1 siRNA - - + +
NT siRNA + + - -
Total Ubiquitin
100 kDa
70 kDa
55 kDa
35 kDa
Mfn2
100 kDa
β-actin
35 kDa

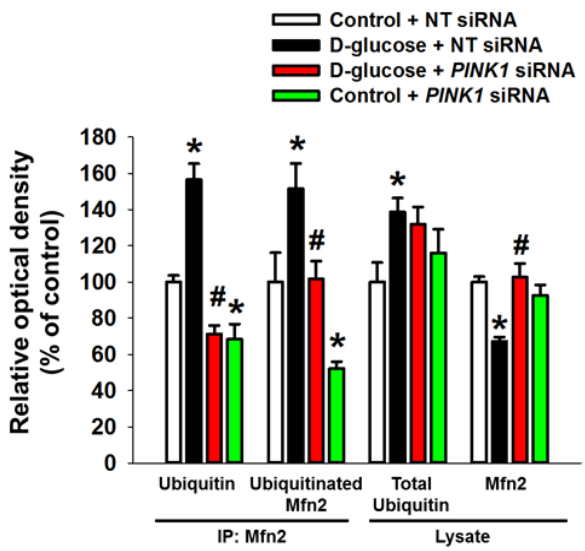
Control + NT siRNA
D-glucose + NT siRNA
D-glucose + PINK1 siRNA
Control + PINK1 siRNA
Relative optical density (% of control)
180
160
140
120
100
80
60
40
20
0
Ubiquitin
Ubiquitinated Mfn2
Total Ubiquitin
Mfn2
IP: Mfn2
Lysate

Figure 7. role of high glucose-induced PINK1 in Mfn2 ubiquitination SK-N-MCs were transfected with PINK1 or NT siRNAs for 24 h prior to D-glucose (25 mM) for 24 h. Mfn2 interacted proteins were immune-precipitated, and blotted with Ubiquitin and Mfn2 antibodies. Cell lysates as an input were blotted with Ubiquitin, Mfn2 and β-actin antibodies. All blot images are representative. Data are showed as a mean ± S.E.M. n = 3. *$p < 0.05$ versus control, #$p < 0.05$ versus D-glucose treatment.

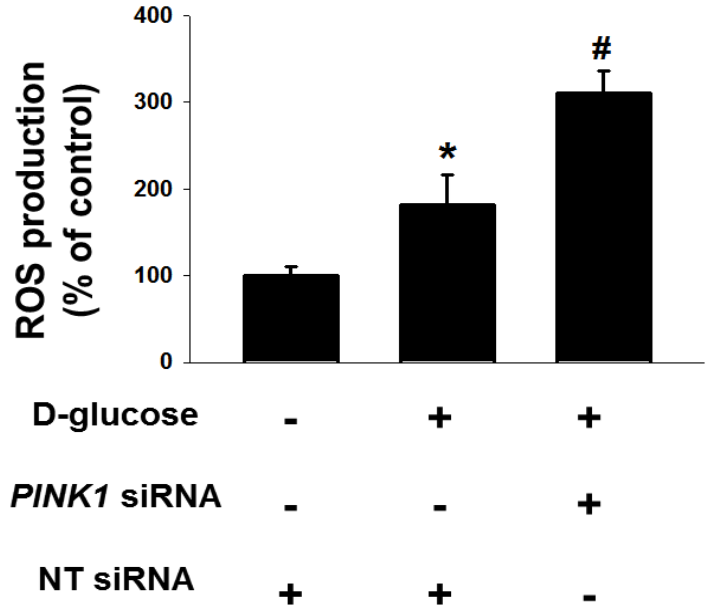

Figure 8. Role of high glucose in ROS accumulation in SK-N-MCs. Cells were transfected with PINK1 siRNA or NT siRNA for 24 h prior to D-glucose (25 mM) treatment for 24 h. Intracellular ROS level was analyzed by DCF-DA staining. The fluorescence intensity of DCF-DA was detected by luminometer. Data are presented as a mean ± S.E.M. n = 6. *p < 0.05 versus control, #p < 0.05 versus D-glucose treatment.

A

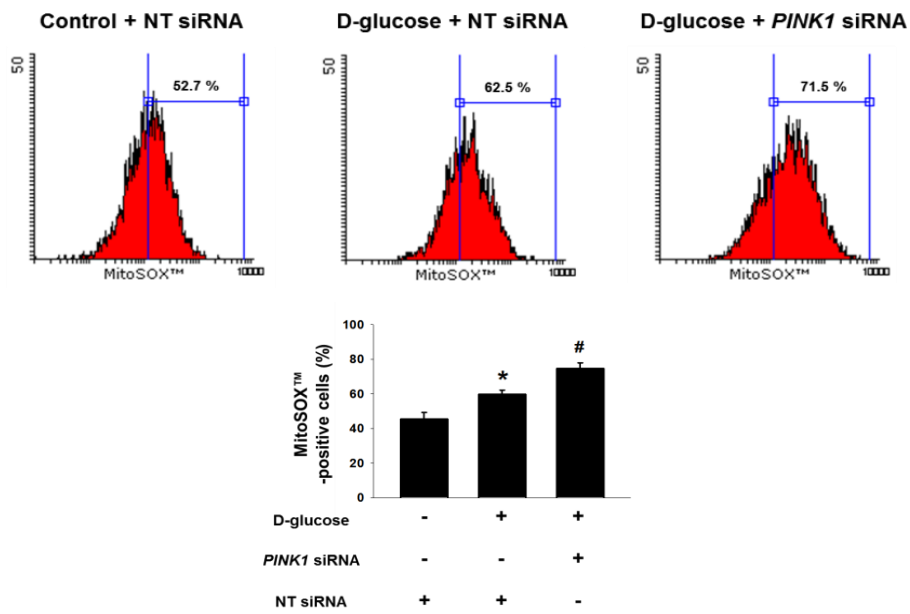
Control + NT siRNA
D-glucose + NT siRNA
D-glucose + PINK1 siRNA
52.7 %
62.5 %
71.5 %
MitoSOX™
MitoSOX™ -positive cells (%)
D-glucose
PINK1 siRNA
NT siRNA

B

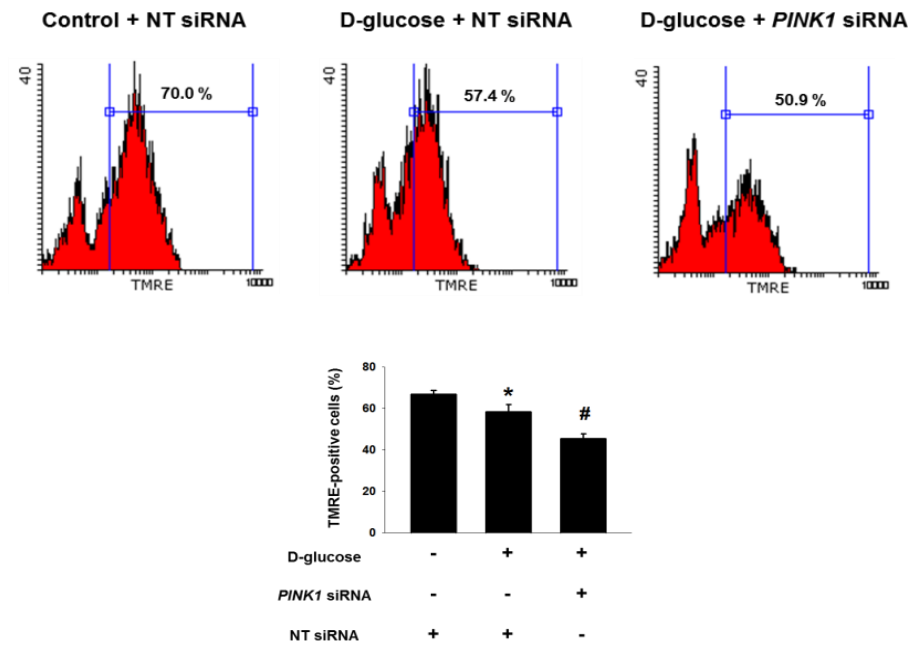
Control + NT siRNA
D-glucose + NT siRNA
D-glucose + PINK1 siRNA
70.0 %
57.4 %
50.9 %
TMRE
TMRE-positive cells (%)
D-glucose
PINK1 siRNA
NT siRNA

Figure 9. Role of PINK1 in the mitochondrial membrane potential in SK-N-MCs under high glucose. (A and B) PINK1 or NT siRNAs were transfected to SK-N-MCs prior to 25 mM of D-glucose treatment for 48 h. The population of MitoSOX™ or TMRE-positive cells was measured by flowcytometer. Data are showed as a mean ± S.E.M. n = 4. *$p < 0.05$ versus control with NT siRNA transfection, #$p < 0.05$ versus D-glucose treatment with NT siRNA transfection.

A

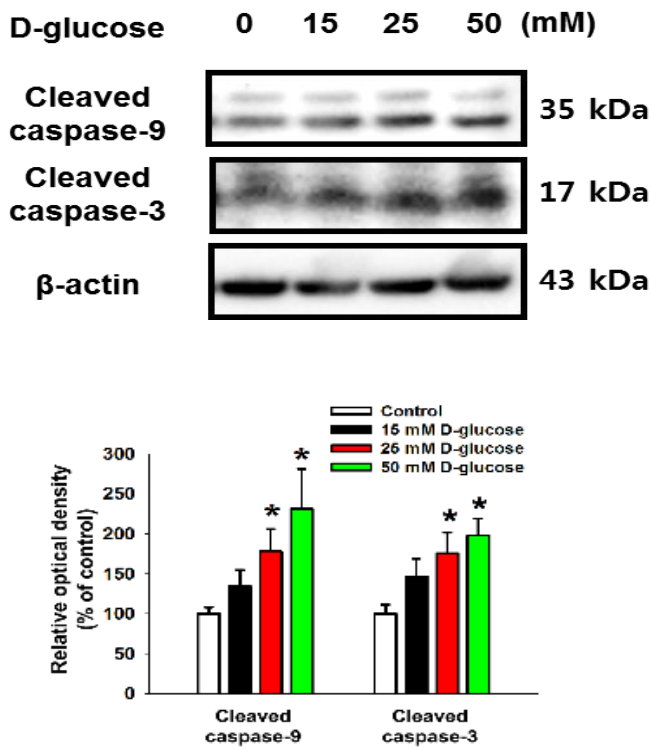
D-glucose 0 15 25 50 (mM)
Cleaved caspase-9
35 kDa
Cleaved caspase-3
17 kDa
β-actin
43 kDa
Control
15 mM D-glucose
25 mM D-glucose
50 mM D-glucose
Relative optical density (% of control)
300
250
200
150
100
50
0
*
Cleaved caspase-9
Cleaved caspase-3

B

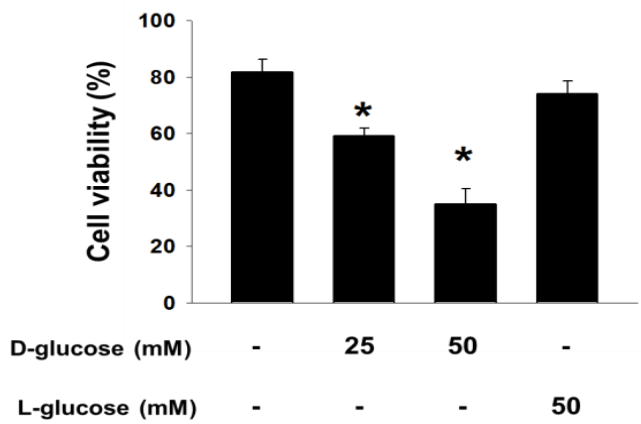
Cell viability (%)
100
80
60
40
20
0
*
D-glucose (mM) - 25 50 -
L-glucose (mM) - - - 50

Figure 10. Role of high glucose-induced PINK1 in neuronal cell death. (A) SK-N-MCs were incubated with the various concentrations of D-glucose (0–50 mM) for 48 h. Cleaved caspase-9, cleaved caspase-3 and β-actin were detected by western blot. ROD data of cleaved caspase-9 and 3 were normalized by β-actin. Quantitative ROD data are presented as a mean ± S.E.M. n = 3. (B) SK-N-MCs were incubated with 25 and 50 mM of D-glucose or 50 mM of L-glucose for 48 h. Cell viability was measured by trypan blue exclusion cell viability assay. Data are presented as a mean ± S.E.M. n = 6. Each blot images are representative. *$p < 0.05$ versus control, #$p < 0.05$ versus D-glucose treatment

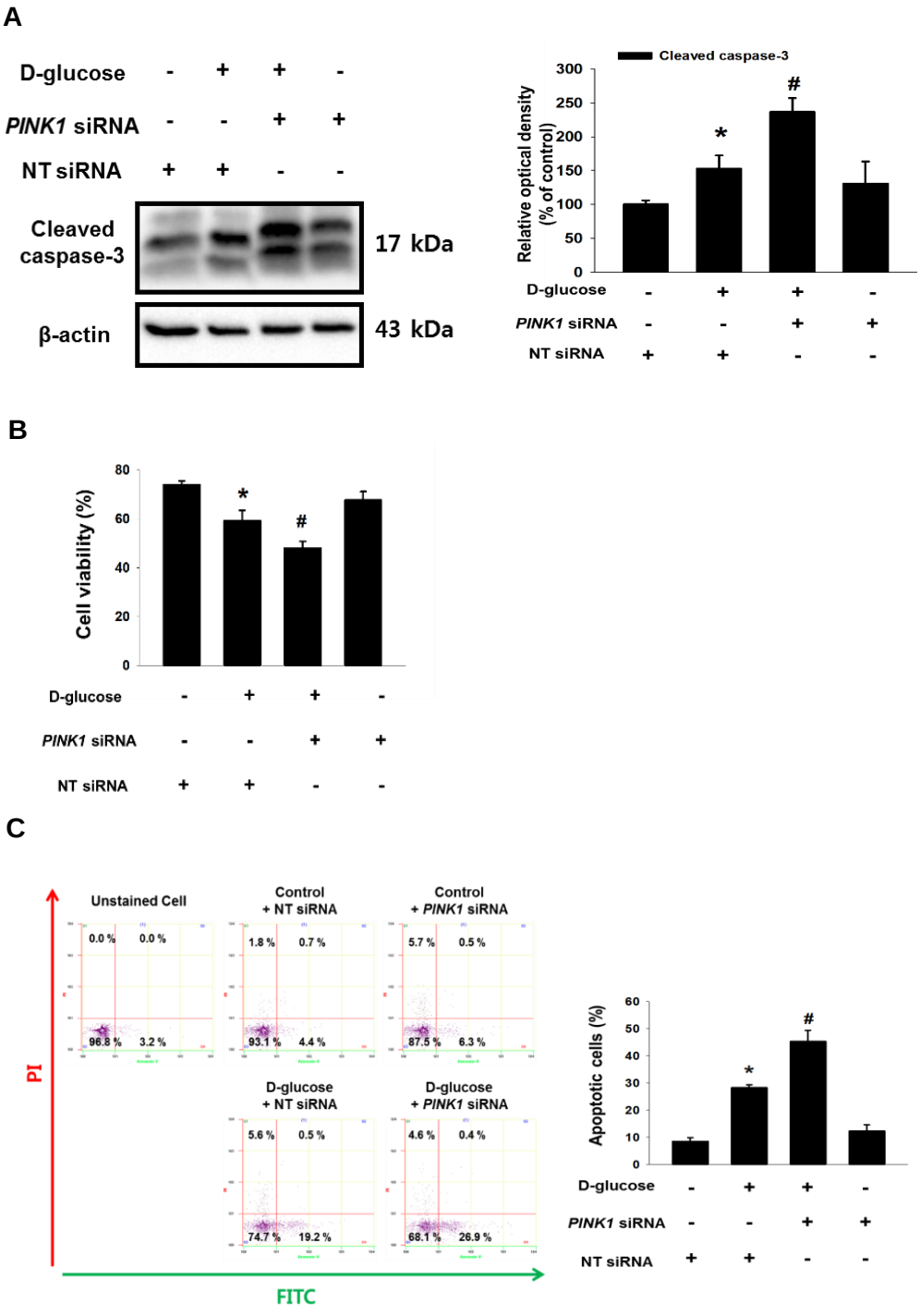
A
D-glucose - + + -
PINK1 siRNA - - + +
NT siRNA + + - -
Cleaved caspase-3
17 kDa
β-actin
43 kDa
Cleaved caspase-3
Relative optical density (% of control)
300
250
200
150
100
50
0
*
#
D-glucose - + + -
PINK1 siRNA - - + +
NT siRNA + + - -
B
Cell viability (%)
80
60
40
20
0
*
#
D-glucose - + + -
PINK1 siRNA - - + +
NT siRNA + + - -
C
Unstained Cell
Control + NT siRNA
Control + PINK1 siRNA
D-glucose + NT siRNA
D-glucose + PINK1 siRNA
0.0 % 0.0 %
96.8 % 3.2 %
1.8 % 0.7 %
93.1 % 4.4 %
5.7 % 0.5 %
87.5 % 6.3 %
5.6 % 0.5 %
74.7 % 19.2 %
4.6 % 0.4 %
68.1 % 26.9 %
PI
FITC
Apoptotic cells (%)
60
50
40
30
20
10
0
*
#
D-glucose - + + -
PINK1 siRNA - - + +
NT siRNA + + - -

Fig. 11 Protective role of PINK1 on high glucose –induce neuronal cell death. (A) PINK1 or NT siRNAs were transfected to SK-N-MCs for 24 h prior to 25 mM of D-glucose treatment for 48 h. Protein expressions of cleaved caspase-9, cleaved caspase-3 and β-actin were measured by western blot. ROD data of cleaved caspase-9 and 3 were normalized by β-actin. Quantitative ROD data are present as a mean ± S.E.M. n = 3. (B) Cell viability was measured by trypan blue exclusion cell viability assay. Data presented as a mean ± S.E.M. n = 6. (C) Apoptotic cells were measured by annexin V/PI analysis assay. Data are reported as a mean ± S.E.M. n = 4. Each blot images are representative. $*p < 0.05$ versus control, $\#p < 0.05$ versus D-glucose treatment.

3. Effect of melatonin on PINK1-mediated mitophagy in neuronal cells

To investigate the effects of melatonin and high glucose on mitophagy regulator expressions in SK-N-MC cells. In those cells, the mRNA expression of PINK1, but not BNIP3 or NIX, was significantly increased by melatonin treatment either with or without high glucose treatment (Fig. 12A). In addition, western blot results showed that melatonin did not affect Parkin, BNIP3, and NIX expressions (Fig. 12B). Moreover, In the present study observed that PINK1 protein expression induced by high glucose was further enhanced by melatonin pretreatment in SK-N-MC and SH-SY5Y cells and in mouse hippocampal neurons (Figs. 13A–13C). Immunofluorescence results showed that COX4 fluorescence intensities in high glucose and after co-treatment of high glucose and melatonin were decreased to 75.5% and 31.6%, respectively, of the untreated level (Fig. 14A). To confirm the effect of melatonin on mitochondrial ROS accumulation and mitochondrial membrane potential, this present study undertook MitoSOX™ and TMRE staining and measured the results by using flow cytometry. As shown in Figures 14B and 14C, melatonin pretreatment

decreased the number of MitoSOX™-positive cells and increased that of TMRE-positive cells. Collectively, present study results indicate that melatonin facilitates PINK1-dependent mitophagy, which is associated with protection against mitochondrial impairment in neuronal cells under high glucose conditions.

A

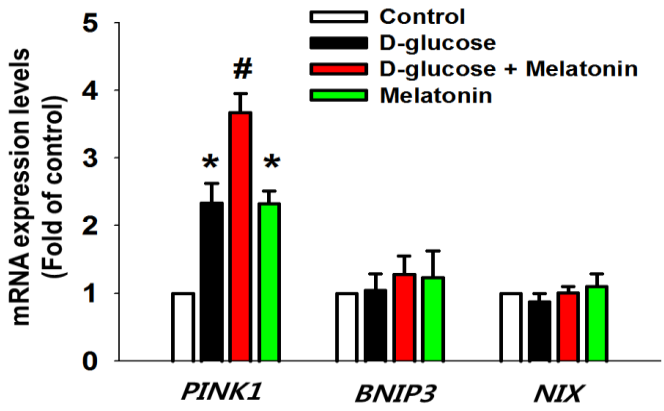
Control
D-glucose
D-glucose + Melatonin
Melatonin
mRNA expression levels
(Fold of control)
5
4
3
2
1
0
#
*
*
PINK1
BNIP3
NIX

B

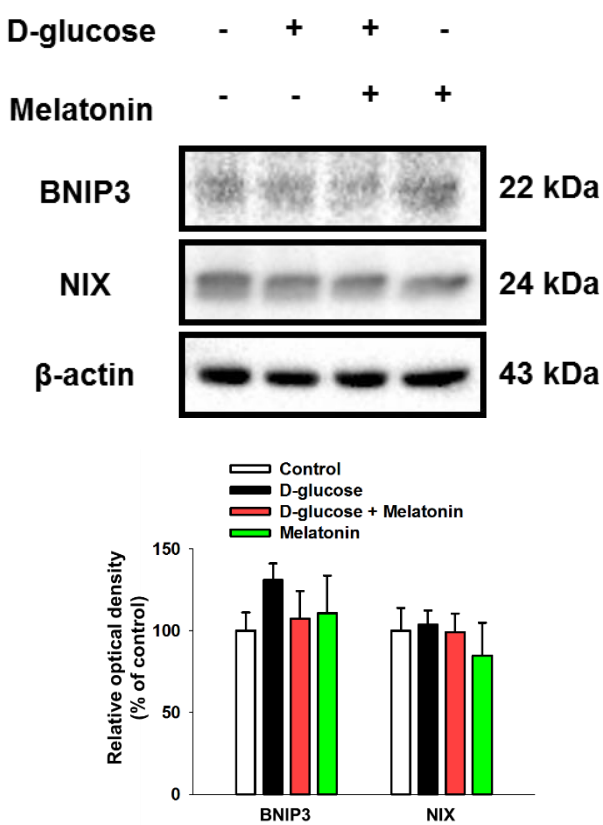
D-glucose - + + -
Melatonin - - + +
BNIP3
22 kDa
NIX
24 kDa
β-actin
43 kDa
Control
D-glucose
D-glucose + Melatonin
Melatonin
Relative optical density
(% of control)
150
100
50
0
BNIP3
NIX

Figure 12. Effect of melatonin on mitophagy regulator expression in neuronal cells under high glucose. (A) SK-N-MCs were incubated with D-glucose (25 mM) and melatonin (1 μM) for 24 h. PINK1, BNIP3, NIX and ACTB mRNA expressions were measured by qPCR. The mRNA expression levels were normalized by ACTB mRNA expression. Data are presented as a mean ± S.E.M. n = 5. (B) SK-N-MCs were incubated with D-glucose (25 mM) and melatonin (1 μM) for 24 h. The protein expressions of BNIP3, NIX and β-actin were analyzed by western blot. ROD data of BNIP3 and NIX were normalized by β-actin. ROD results are showed as a mean ± S.E.M. n = 3. Each blot images are representative. *$p < 0.05$ versus control, #$p < 0.05$ versus D-glucose treatment.

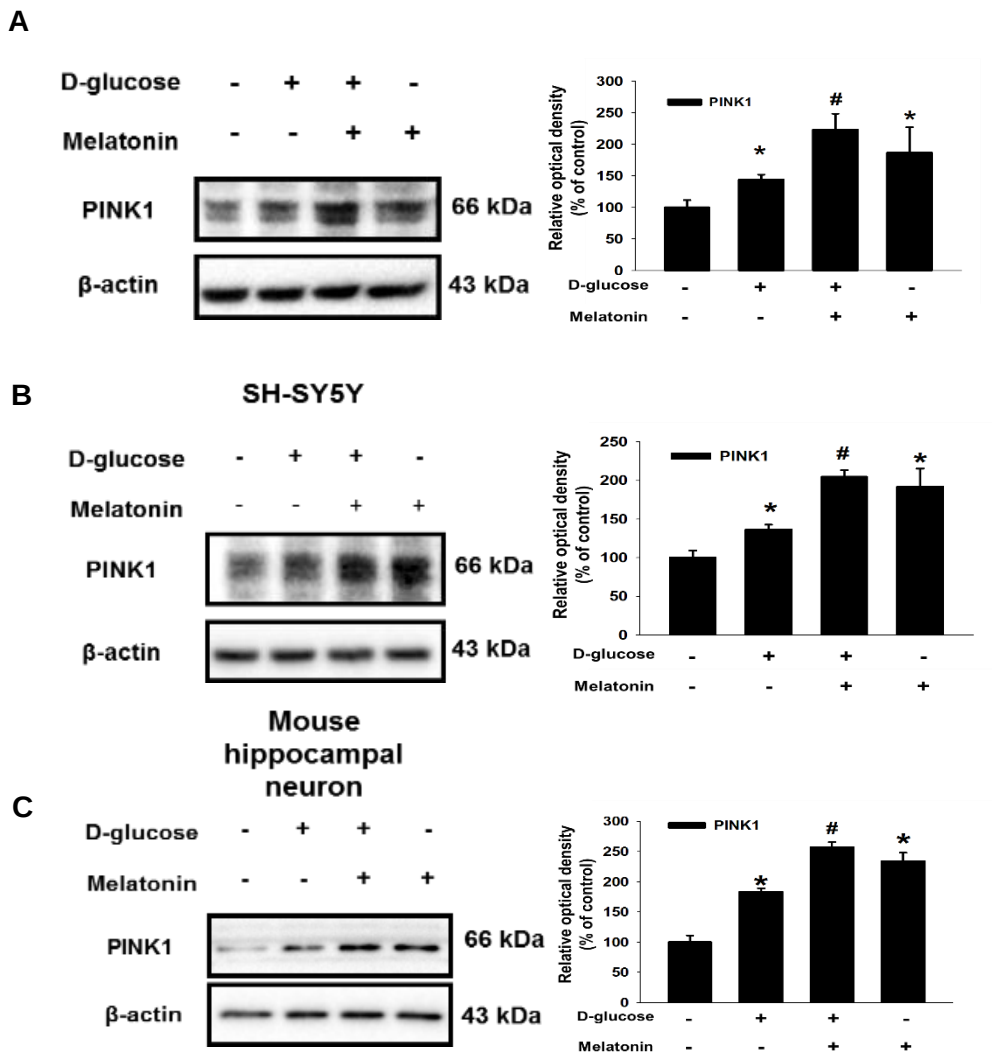

Figure 13. Effect of melatonin on PINK1 expression in neuronal cells under high glucose.

(A-C) SK-N-MCs, SHSY-5Ys and mouse primary hippocampal neurons were incubated with 25 mM of D-glucose and melatonin (1 μM) for 24 h. PINK1 and β-actin protein expressions were analyzed by western blot. ROD data of PINK1 was normalized by β-actin. Quantitative ROD data are present as a mean ± S.E.M. n = 4. *$p < 0.05$ versus control, #$p < 0.05$ versus D-glucose treatment.

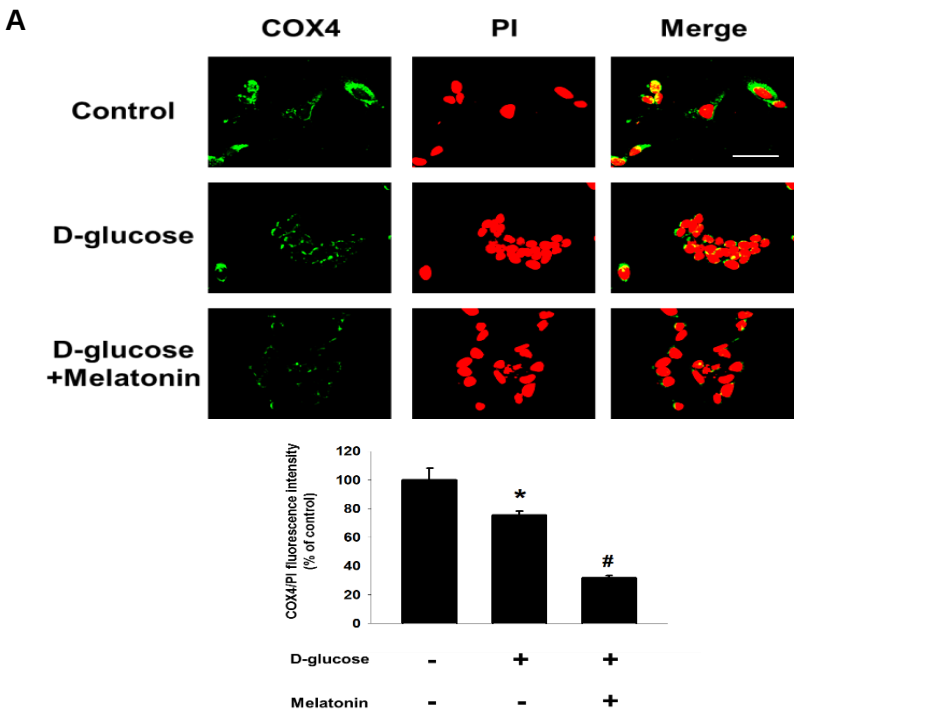
A
COX4
PI
Merge
Control
D-glucose
D-glucose
+Melatonin
COX4/PI fluorescence intensity
(% of control)
120
100
80
60
40
20
0
*
#
D-glucose - + +
Melatonin - - +

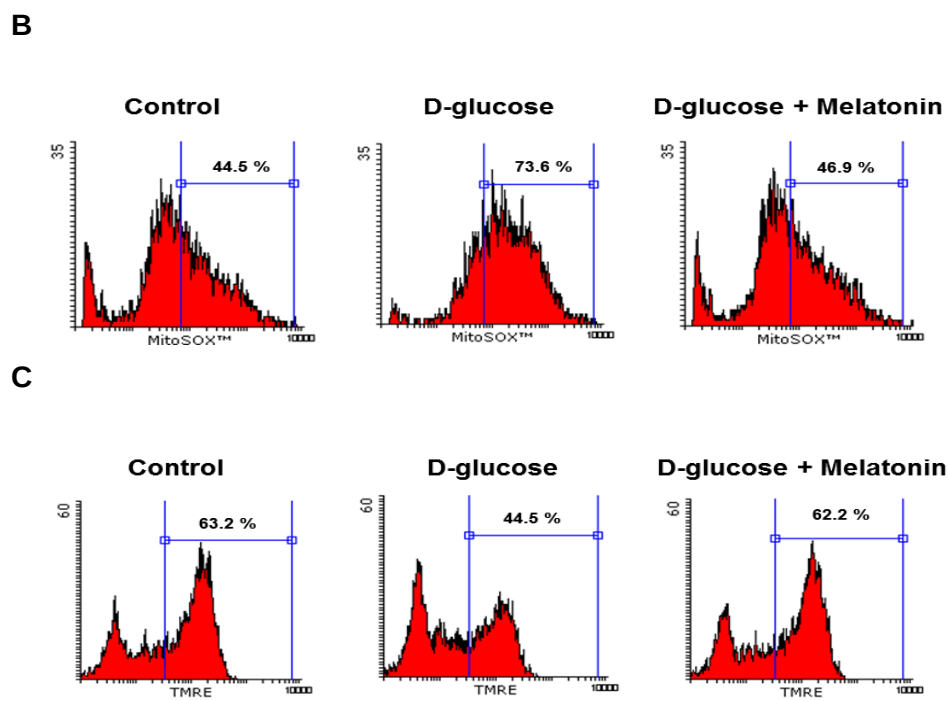
B
Control
D-glucose
D-glucose + Melatonin
35
44.5 %
73.6 %
46.9 %
MitoSOX™
C
Control
D-glucose
D-glucose + Melatonin
60
63.2 %
44.5 %
62.2 %
TMRE

Figure 14. Effect of melatonin on mitochondrial function in neuronal cells under high glucose. (A) SK-N-MCs were incubated with D-glucose (25 mM) and melatonin (1 μM) for 24 h. Cells were immunostained with COX4-specific antibody and PI.The fluorescence intensities of COX4 was presented as a mean ± S.E.M. n = 6 (magnification, ×800). All scale bars, 10 μm. All confocal images are representative. (B, C) SK-N-MCs were incubated with D-glucose (25 mM) and melatonin (1 μM) for 48 h. Cells were stained with MitoSOX™ or TMRE. The population of MitoSOX™ or TMRE-positive cells was measured by flowcytometer. Data are showed as a mean ± S.E. n = 4. *$p < 0.05$ versus control, #$p < 0.05$ versus D-glucose treatment.

4. Involvement of MT_2/Akt/NF-κB pathway in PINK1 induction by melatonin

To investigated the mechanism involved in melatonin regulation of PINK1 expression in neuronal cells. Present study observed the mRNA expressions of melatonin receptors MTNR1A and MTNR1B, in SK-N-MC cells (Fig. 15). To confirm the effect of high glucose on melatonin receptor mRNA expressions, this present study incubated SK-N-MC cells with different concentrations of D-glucose and observed that 25 and 50 mM of D-glucose stimulated MTNR1B mRNA expression, which was reversed by pretreatment with ROS scavenger NAC (Fig 15B-15D). Therefore, this present study focused on the role of MTNR1B in melatonin-induced PINK1 expression. As shown in the figures 16A–16C, PINK1 expression induced by melatonin (1 μM) was abolished by pretreatment with the MT_2 specific inhibitor 4-P-PDOT in SK-N-MC and SH-SY5Y cells and in mouse hippocampal neurons. Based upon these results suggest that high glucose induces MT_2 expression via ROS signaling, and such expression is critical for melatonin's action on PINK1 expression. This present study also checked 4-P-PDOT's effect on PINK1 expression as a control in SK-

M-MC, SH-SY5Y and mouse hippocampal neuron. And, present study data showed that pretreatment of 4-P-PDOT did not affect high glucose-induced PINK1 expression in SK-M-MC, SH-SY5Y and mouse hippocampal neuron (Figs. 17A-17C). Further study investigated the signaling pathway regulating PINK1 expression induced by MT_2 activation. The results showed that phosphorylation of Akt at the Thr389 and Ser473 residues increased to the greatest extent after 24 h of D-glucose treatment (Fig. 18A). High glucose-phosphorylation of Akt, but not ERK or pan PKC, was further augmented by melatonin treatment (Fig. 18B and Fig. 18C). This present study data showed that high glucose treatment stimulated NF-κB phosphorylation at the Ser536 residue, with a further increase induced by melatonin treatment (Fig. 19A). Melatonin treatment stimulated expressions of phosphorylated NF-κB and total NF-κB in the nucleus (Fig. 19B). Furthermore, this study also found that pretreatment of PI3K inhibitor LY294002 abolished enhancement of phosphorylation and nuclear translocation of NF-κB by melatonin (Figs. 19A and 19B). To confirm the role of NF-κB activated by high glucose or melatonin in PINK1 expression, this present study pretreated NF-κB inhibitor SN-50 to melatonin-pretreated SK-N-MC cells. The

results showed that enhanced mRNA and protein expressions of PINK1 by melatonin treatment were decreased by SN-50 (Figs. 20A and 20B). Consistent with those results, present study observed induction of PINK1 by melatonin in SH-SY5Y cells (Fig. 20C). Based upon findings, this present study suggest that melatonin facilitates high glucose induction of Akt/NF-κB signaling via MT_2 activation, thereby leading to PINK1 expression.

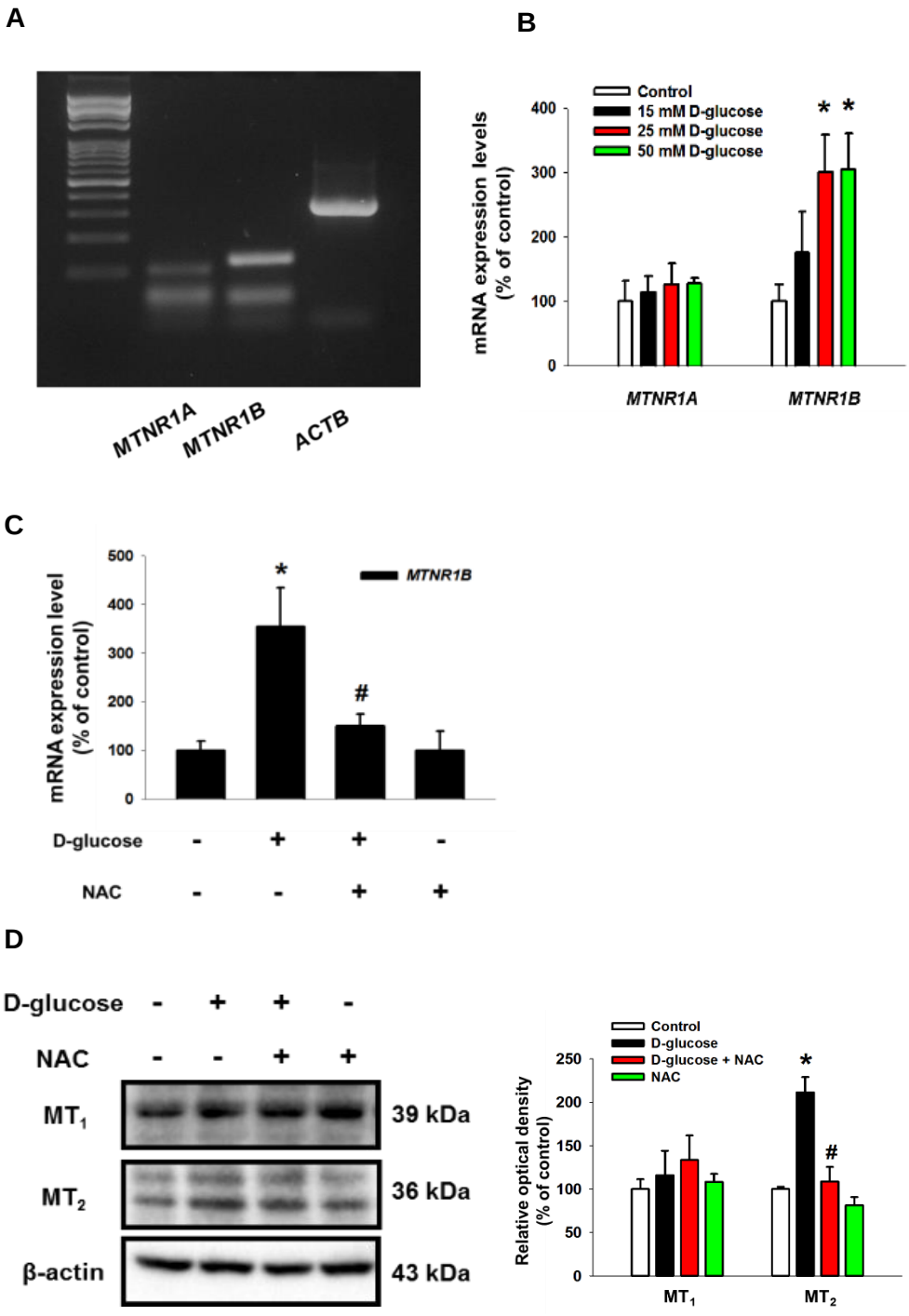
A
MTNR1A
MTNR1B
ACTB
B
Control
15 mM D-glucose
25 mM D-glucose
50 mM D-glucose
mRNA expression levels (% of control)
400
300
200
100
0
* *
MTNR1A
MTNR1B
C
MTNR1B
mRNA expression level (% of control)
500
400
300
200
100
0
*
#
D-glucose - + + -
NAC - - + +
D
D-glucose - + + -
NAC - - + +
MT1
MT2
β-actin
39 kDa
36 kDa
43 kDa
Control
D-glucose
D-glucose + NAC
NAC
Relative optical density (% of control)
250
200
150
100
50
0
*
#
MT1
MT2

Figure 15. Effect of high glucose on melatonin receptors' mRNA expression. (A) Harboring of MTNR1A and MTNR1B mRNA in SK-N-MCs. mRNA expressions of MTNR1A, MTNR1B and ACTB in SK-N-MCs were showed with PCR. (B) SK-N-MCs were exposed to various concentrations of D-glucose (0-50 mM). MTNR1A, MTNR1B and ACTB mRNA expressions were detected by qPCR. The mRNA expression levels of MTNR1A and MTNR1B were normalized by ACTB mRNA expression. Quantitative data are presented as a mean ± S.E.M. n = 5. (C) SK-N-MCs were pretreated with NAC (5 mM) for 30 min prior to treatment of D-glucose (25 mM) for 24 h. MTNR1B and ACTB mRNA expressions were detected by qPCR. The mRNA expression levels of MTNR1B were normalized by ACTB mRNA expression. Data are presented as a mean ± S.E.M. n = 5. (D) The protein expressions of MT_1, MT_2 and β-actin were measured by western blot. Quantitative ROD data are present as a mean ± S.E.M. n = 3. *$p < 0.05$ versus control, #$p < 0.05$ versus D-glucose treatment, @$p < 0.05$ versus co-treatment of D-glucose and melatonin.

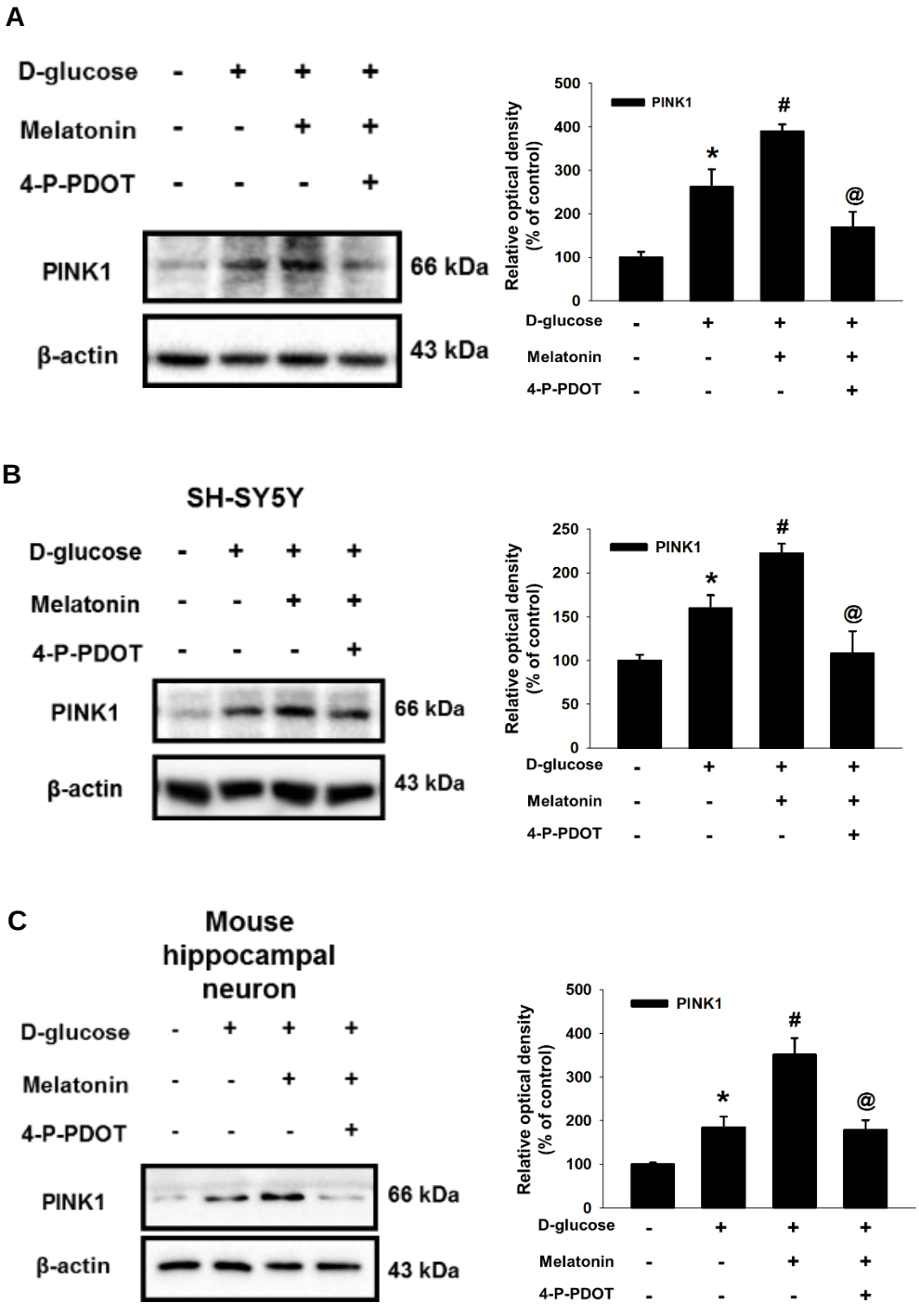
A
D-glucose - + + +
Melatonin - - + +
4-P-PDOT - - - +
PINK1
β-actin
66 kDa
43 kDa
Relative optical density (% of control)
PINK1
*
#
@
B
SH-SY5Y
C
Mouse hippocampal neuron

Figure 16, Role of MT_2 signaling activated by melatonin in high glucose-induced PINK1 expression. (A–C) SK-N-MCs, SHSY-5Y and mouse hippocampal neurons were pretreated with D-glucose (25 mM) and 4-P-PDOT (10 nM) for 30 min prior to melatonin (1 μM) treatment for 24 h. PINK1 and β-actin protein expressions were analyzed by western blot. Data represent as a mean ± S.E.M. n = 3. *$p < 0.05$ versus control, #$p < 0.05$ versus D-glucose treatment, @$p < 0.05$ versus co-treatment of D-glucose and melatonin.

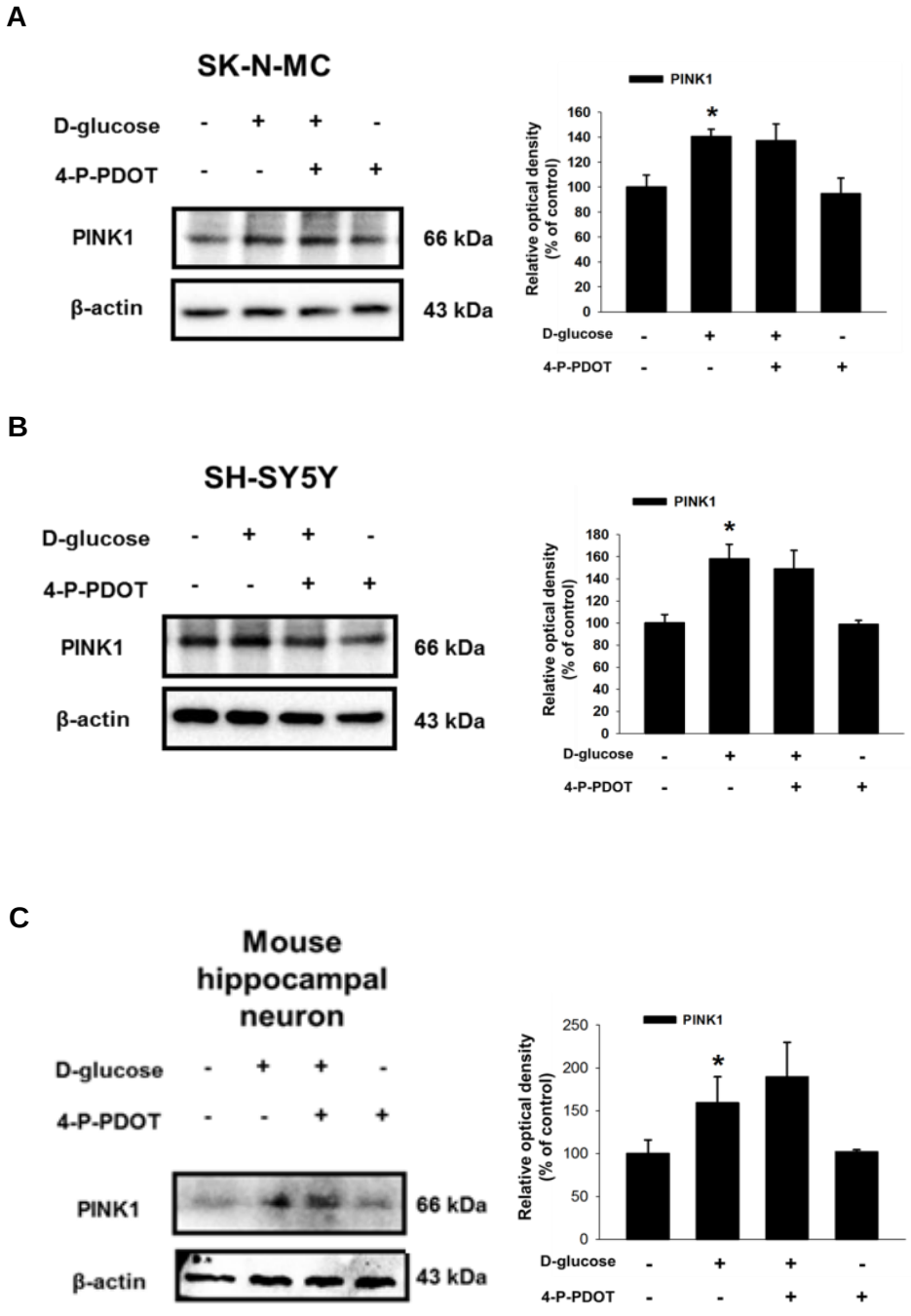
A
SK-N-MC
D-glucose - + + -
4-P-PDOT - - + +
PINK1
66 kDa
β-actin
43 kDa
PINK1
Relative optical density (% of control)
160
140
120
100
80
60
40
20
0
*
D-glucose - + + -
4-P-PDOT - - + +
B
SH-SY5Y
D-glucose - + + -
4-P-PDOT - - + +
PINK1
66 kDa
β-actin
43 kDa
PINK1
Relative optical density (% of control)
180
160
140
120
100
80
60
40
20
0
*
D-glucose - + + -
4-P-PDOT - - + +
C
Mouse hippocampal neuron
D-glucose - + + -
4-P-PDOT - - + +
PINK1
66 kDa
β-actin
43 kDa
PINK1
Relative optical density (% of control)
250
200
150
100
50
0
*
D-glucose - + + -
4-P-PDOT - - + +

Figure 17. Effect of 4-P-PDOT on the PINK1 expression in neuronal cells. (A-C) SK-N-MC, SH-SY5Y and mouse hippocampal neuron were pretreated with 4-P-PDOT (10 μM) prior to D-glucose (25 mM) for 24 h. PINK1 and β-actin expressions were analyzed by western blot. All blot images are representative. Data are present as a mean ± S.E.M. n = 3. *$p < 0.05$ versus control.

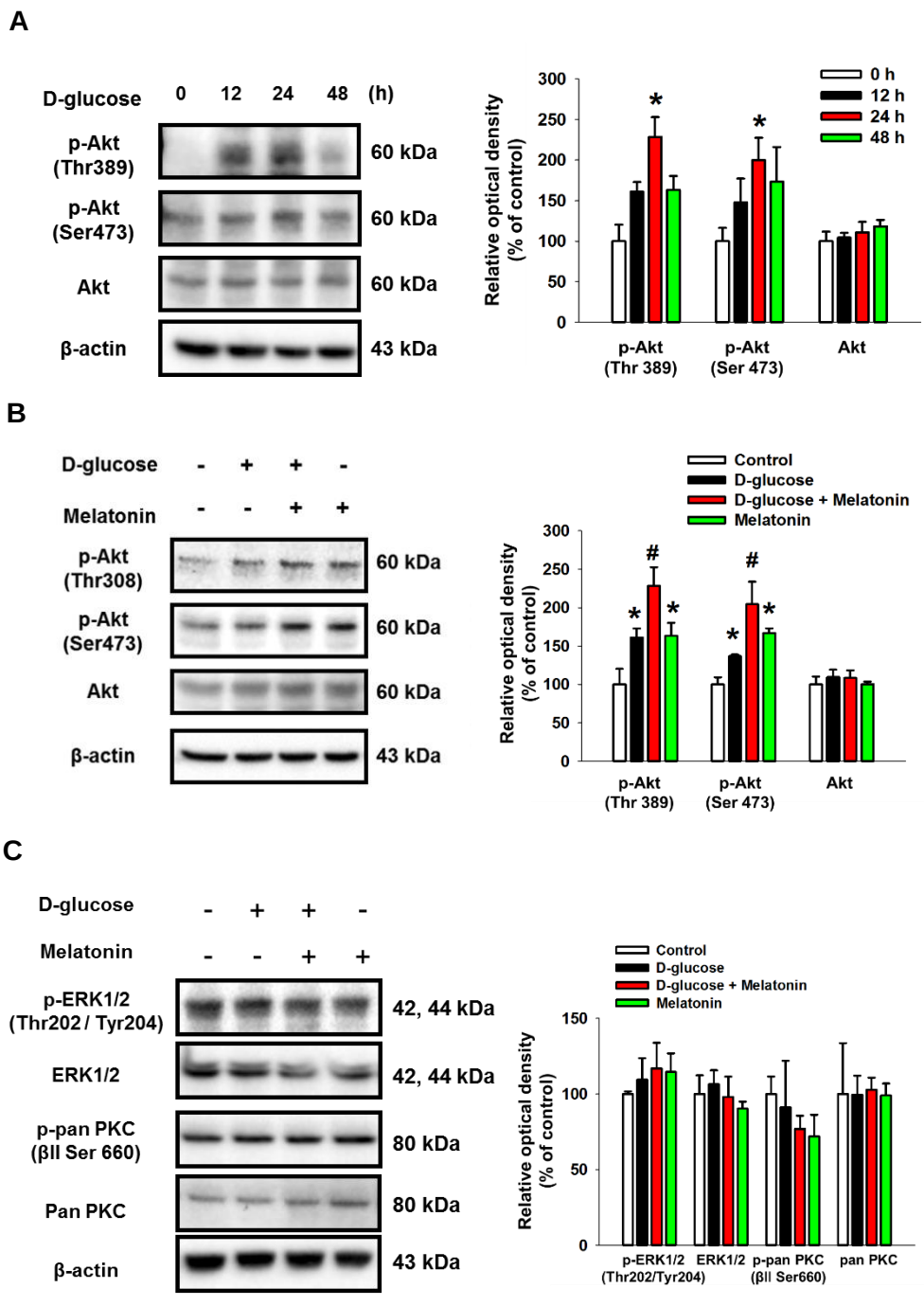
A
D-glucose 0 12 24 48 (h)
p-Akt (Thr389)
p-Akt (Ser473)
Akt
β-actin
60 kDa
60 kDa
60 kDa
43 kDa
Relative optical density (% of control)
0 h
12 h
24 h
48 h
p-Akt (Thr 389)
p-Akt (Ser 473)
Akt
B
D-glucose - + + -
Melatonin - - + +
p-Akt (Thr308)
p-Akt (Ser473)
Akt
β-actin
60 kDa
60 kDa
60 kDa
43 kDa
Control
D-glucose
D-glucose + Melatonin
Melatonin
C
D-glucose - + + -
Melatonin - - + +
p-ERK1/2 (Thr202 / Tyr204)
ERK1/2
p-pan PKC (βII Ser 660)
Pan PKC
β-actin
42, 44 kDa
42, 44 kDa
80 kDa
80 kDa
43 kDa
p-ERK1/2 (Thr202/Tyr204)
ERK1/2
p-pan PKC (βII Ser660)
pan PKC

Figure 18. Effect of melatonin on AKT, ERK and PKC phosphorylation in SK-N-MC under high glucose condition. (A) SK-N-MCs were incubated with various durations of D-glucose (25 mM) treatment. The protein expressions of p-Akt (Thr389), p-Akt (Ser473), Akt and β-actin were analyzed by western blot. ROD data are present as a mean ± S.E.M. n = 4. (B) SK-N-MCs were incubated with D-glucose (25 mM) and melatonin (1 μM) for 24 h. The protein expressions of p-Akt (Thr389), p-Akt (Ser473), Akt and β-actin were analyzed by western blot. ROD data are present as a mean ± S.E.M. n = 4. (C) SK-N-MCs were incubated with D-glucose (25mM) and melatonin (1 μM) for 24 h. The protein expressions of p-ERK (Thr202 / Tyr204), ERK1/2, p-pan PKC (βII Ser660), Total PKC and β-actin were analyzed by western blot. ROD data of p-ERK (Thr202 / Tyr204), ERK1/2, p-pan PKC (βII Ser660), Total PKC were normalized by β-actin. ROD result are presented as a mean ± S.E.M. n = 3. Each blot images are representative. *$p < 0.05$ versus control, #$p < 0.05$ versus D-glucose treatment, @$p < 0.05$ versus co-treatment of D-glucose and melatonin

A

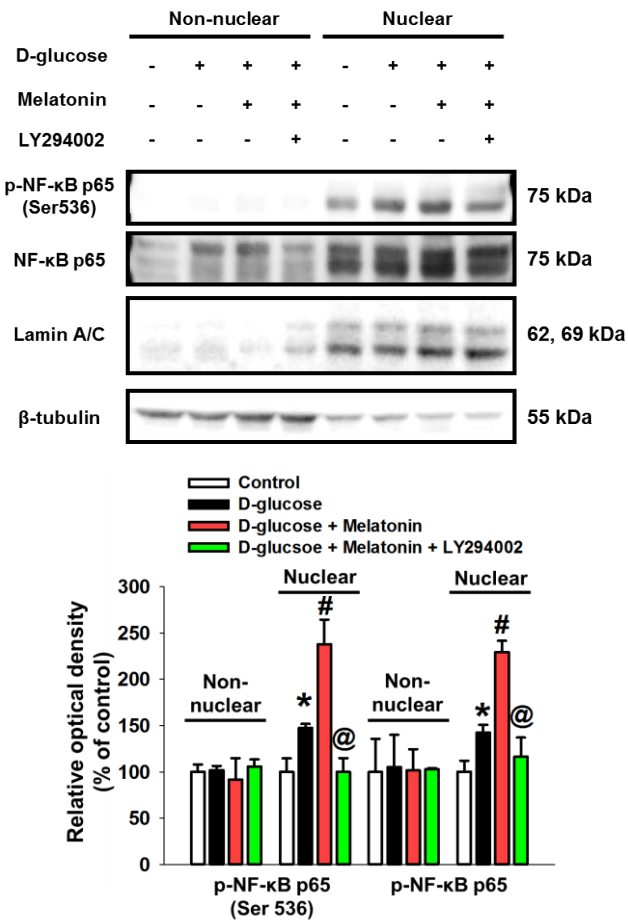
Non-nuclear
Nuclear
D-glucose
Melatonin
LY294002
p-NF-κB p65 (Ser536)
75 kDa
NF-κB p65
75 kDa
Lamin A/C
62, 69 kDa
β-tubulin
55 kDa
Control
D-glucose
D-glucose + Melatonin
D-glucsoe + Melatonin + LY294002
Relative optical density (% of control)
Non-nuclear
Nuclear
p-NF-κB p65 (Ser 536)
p-NF-κB p65

B

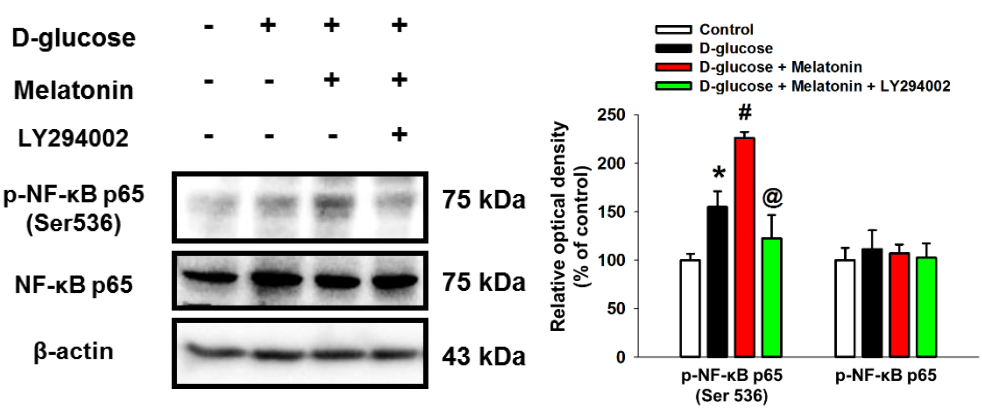
D-glucose
Melatonin
LY294002
p-NF-κB p65 (Ser536)
75 kDa
NF-κB p65
75 kDa
β-actin
43 kDa
Control
D-glucose
D-glucose + Melatonin
D-glucose + Melatonin + LY294002
Relative optical density (% of control)
p-NF-κB p65 (Ser 536)
p-NF-κB p65

Figure 19. Effect of glucose and melatonin on nuclear factor kappa-light-chain-enhancer of activated B cells (NF-κB) phosphorylation in SK-N-MC (A) SK-N-MCs were pretreated with D-glucose (25 mM) and LY294002 (1 μM) for 30 min prior to melatonin (1 μM) treatment for 24 h. The protein expressions of p-NF-κB p65 (Ser 536), NF-κB, β-actin were detected by western blot. ROD data are present as a mean ± S.E.M. n = 4. (B) The protein expressions of p-NF-κB p65 (Ser536), NF-κB p65, lamin A/C and β-tubulin were analyzed by western blot. Lamin A/C and β-tubulin were used as a nuclear and non-nuclear protein controls, respectively. Data are presented as a mean ± S.E.M. n = 4. Each blot images are representative. *$p < 0.05$ versus control, #$p < 0.05$ versus D-glucose treatment, @$p < 0.05$ versus co-treatment of D-glucose and melatonin

A

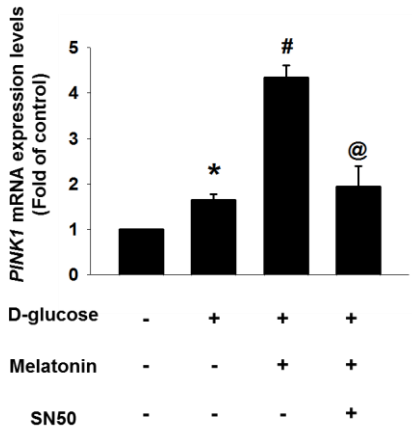
PINK1 mRNA expression levels
(Fold of control)
5
4
3
2
1
0
*
#
@
D-glucose - + + +
Melatonin - - + +
SN50 - - - +

B

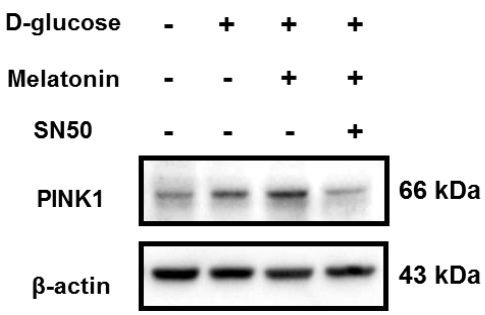
D-glucose - + + +
Melatonin - - + +
SN50 - - - +
PINK1
66 kDa
β-actin
43 kDa

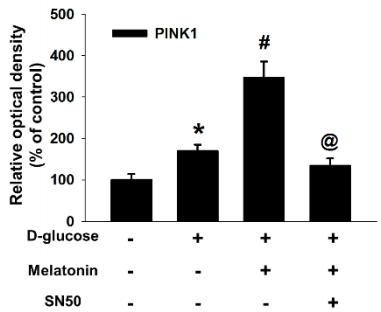
PINK1
Relative optical density
(% of control)
500
400
300
200
100
0
*
#
@
D-glucose - + + +
Melatonin - - + +
SN50 - - - +

C

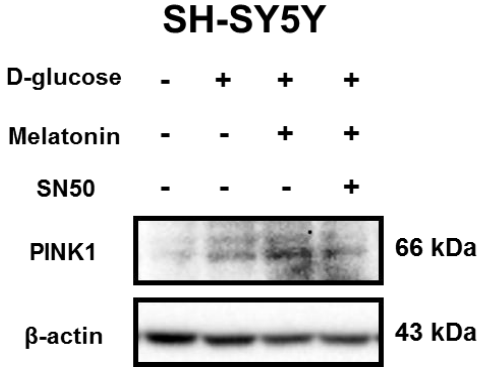
SH-SY5Y
D-glucose - + + +
Melatonin - - + +
SN50 - - - +
PINK1
66 kDa
β-actin
43 kDa

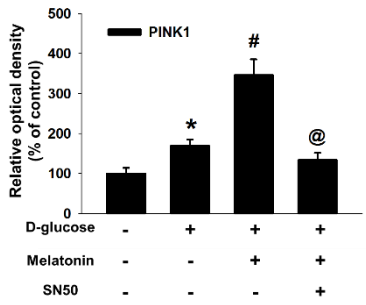
PINK1
Relative optical density
(% of control)
500
400
300
200
100
0
*
#
@
D-glucose - + + +
Melatonin - - + +
SN50 - - - +

Figure 20. Role of NF-κB activated by high glucose or melatonin in PINK1 expression.

(A) SK-N-MCs were pretreated with D-glucose (25 mM) and SN50 (5 μM) for 30 min prior to melatonin (1 μM) treatment for 24 h. PINK1 and ACTB mRNA expressions were analyzed by qPCR. The mRNA expression level of PINK1 was normalized by ACTB mRNA expression. Quantitative data are presented as a mean ± S.E.M. n = 5. (B and C) SK-N-MCs and SHSY-5Ys were pretreated with D-glucose (25 mM) and SN50 (5 μM) for 30 min prior to melatonin (1 μM) treatment for 24 h. The protein expressions of PINK1 and β-actin were detected by western blot. ROD data of PINK1 were normalized by β-actin. Data are presented as a mean ± S.E.M. n = 4. Each blot images are representative. *$p < 0.05$ versus control, #$p < 0.05$ versus D-glucose treatment, @$p < 0.05$ versus co-treatment of D-glucose and melatonin.

5. Effect of PINK1 induced by melatonin on neuronal cell death

To determine the effect of melatonin-induced PINK1 expression on neuronal cell death under high glucose conditions, this present study investigated ROS regulation and neuronal cell apoptosis by assessing PINK1 siRNA transfection and melatonin in SK-N-MC cells with high glucose treatment. As shown in Figure 16A, the reduced intracellular ROS level in high glucose-incubated SK-N-MC cells induced by melatonin treatment was recovered by PINK1 siRNA transfection. In addition, the increase in caspase-9 and -3 expressions induced by high glucose were significantly reversed by melatonin treatment, and reversed by PINK1 siRNA transfection in SK-N-MC cells (Fig. 16B). Trypan blue exclusion assay results showed that cell viability of NT siRNA-transfected SK-N-MC cells given high glucose and melatonin treatments was higher than that of NT siRNA-transfected SK-N-MC cells given high glucose alone. Moreover, this protective effect of melatonin against SK-N-MC cell apoptosis induced by high glucose was significantly reduced by PINK1 siRNA transfection (Fig. 17A). Likewise, annexin V/propidium iodide (PI) staining flow cytometry

results showed that melatonin significantly decreased the number of annexin V-positive cells in SK-N-MC cells treated with high glucose, reversed by PINK1 siRNA transfection (Fig. 17B). Taken together, the present study results indicate that PINK1 has a crucial role in the anti-apoptotic effect of melatonin in neuronal cells.

A

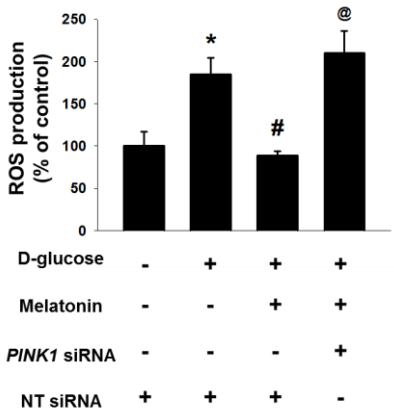
ROS production
(% of control)
250
200
150
100
50
0
*
#
@
D-glucose - + + +
Melatonin - - + +
PINK1 siRNA - - - +
NT siRNA + + + -

B

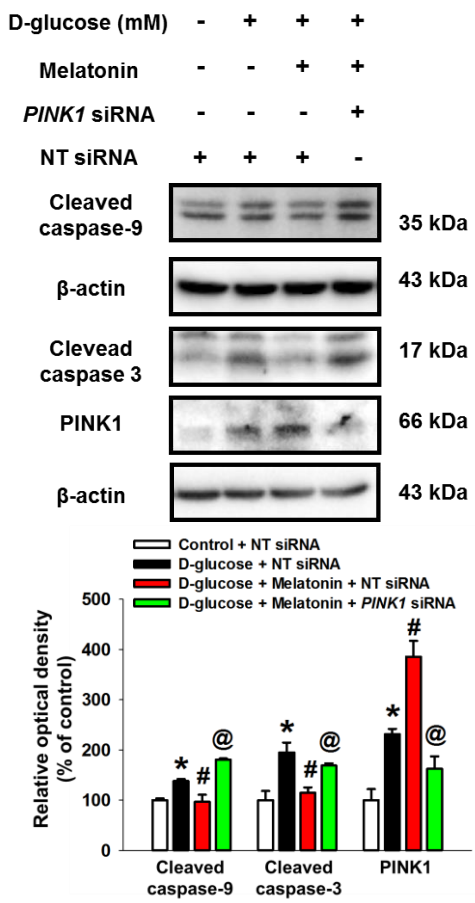
D-glucose (mM) - + + +
Melatonin - - + +
PINK1 siRNA - - - +
NT siRNA + + + -
Cleaved caspase-9
35 kDa
β-actin
43 kDa
Clevead caspase 3
17 kDa
PINK1
66 kDa
β-actin
43 kDa
Control + NT siRNA
D-glucose + NT siRNA
D-glucose + Melatonin + NT siRNA
D-glucose + Melatonin + PINK1 siRNA
Relative optical density
(% of control)
500
400
300
200
100
0
Cleaved caspase-9
Cleaved caspase-3
PINK1

Figure. 21. Effect of melatonin-induced PINK1 expression on ROS regulation and SK-N-MC cells apoptosis under high glucose conditions. (A) PINK1 specific and NT siRNAs were transfected to SK-N-MCs for 24 h prior to D-glucose (25 mM) and melatonin (1 μM) for 48 h. Intracellular ROS level was measured by using DCF-DA staining. The fluorescence intensity of DCF-DA was detected by using luminometer. Data are presented as a mean ± S.E.M. n = 6. (B) The protein expressions of cleaved caspase-9, cleaved caspase-3, PINK1 and β-actin were analyzed by western blot. The ROD data of cleaved caspase-9, cleaved caspase-3, PINK1 were normalized by β-actin. Each blot images are representative. $p < 0.05$ versus control with NT siRNA transfection, #$p < 0.05$ versus D-glucose treatment with NT siRNA transfection, @$p < 0.05$ versus co-treatment of D-glucose and melatonin with NT siRNA transfection.

A

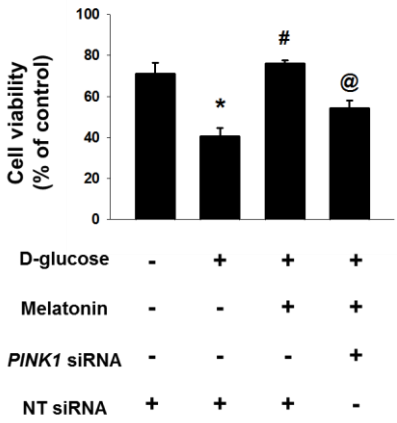
Cell viability
(% of control)
100
80
60
40
20
0
*
#
@
D-glucose - + + +
Melatonin - - + +
PINK1 siRNA - - - +
NT siRNA + + + -

B

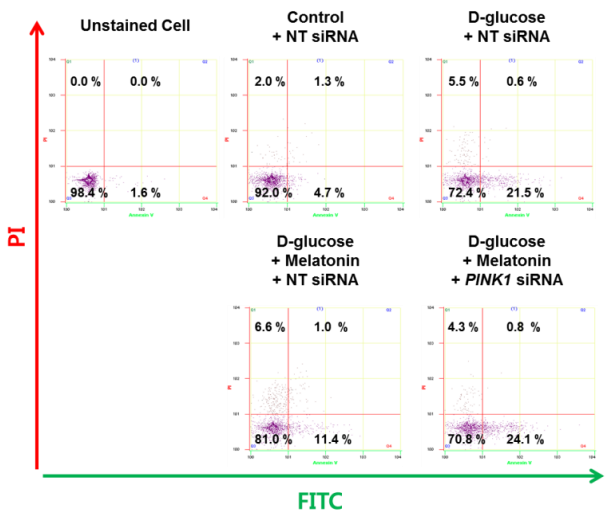
Unstained Cell
Control
+ NT siRNA
D-glucose
+ NT siRNA
0.0 %
0.0 %
98.4 %
1.6 %
2.0 %
1.3 %
92.0 %
4.7 %
5.5 %
0.6 %
72.4 %
21.5 %
D-glucose
+ Melatonin
+ NT siRNA
D-glucose
+ Melatonin
+ PINK1 siRNA
6.6 %
1.0 %
81.0 %
11.4 %
4.3 %
0.8 %
70.8 %
24.1 %
PI
FITC

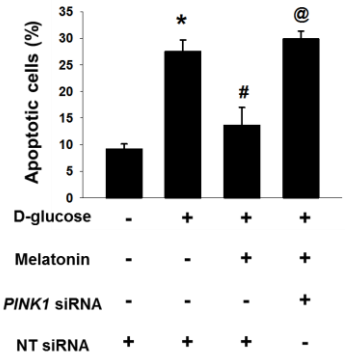
Apoptotic cells (%)
35
30
25
20
15
10
5
0
*
#
@
D-glucose - + + +
Melatonin - - + +
PINK1 siRNA - - - +
NT siRNA + + + -

Figure 22. Protective role of PINK1 expression enhanced by melatonin in high glucose-induced apoptosis in SK-N-MCs. (A) PINK1 specific and NT siRNAs were transfected to SK-N-MCs for 24 h prior to D-glucose (25 mM) and melatonin (1 μM) for 48 h. Cell viability was analyzed by trypan blue exclusion cell viability assay. Data presented as a mean ± S.E.M. n = 6. (B) Apoptotic cells were measured by annexin V/PI analysis assay. Data are reported as a mean ± S.E.M. n = 4. *$p < 0.05$ versus control with NT siRNA transfection, #$p < 0.05$ versus D-glucose treatment with NT siRNA transfection, @$p < 0.05$ versus co-treatment of D-glucose and melatonin with NT siRNA transfection.

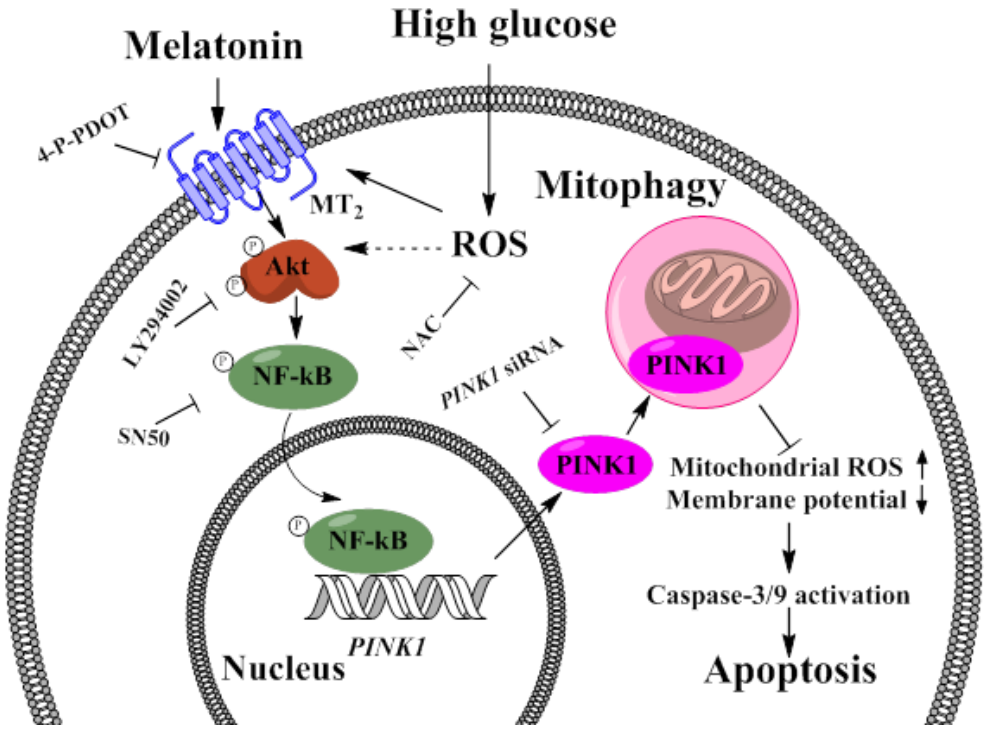

Figure 23. Schematic model of for mechanism involved in the regulatory role of melatonin in high glucose-induced PINK1 expression and neuronal cell survival.

DISCUSSION

The results of this study highlight the mechanism of PINK1 regulation by melatonin in high glucose-induced neuronal cell death. Many investigators have reported that mitophagy is increased in various in vitro and in vivo DM models (Hoshino et al., 2014; Moruno et al., 2012; Stovring et al., 2013; Tang et al., 2015). In addition, previous research has presented evidence of relationships between PINK1 variation and T2DM-induced neurodegeneration (Scheele et al., 2007). Although the majority of previous reports focused on PINK1 regulation by high glucose (Huang et al., 2016; Tang et al., 2015), a recent report showed that high glucose also increases BNIP3 expression, which contributes to cell survival in myocardial cells (Zhou et al., 2015). Present study has demonstrated that high glucose stimulates PINK1 expression, but not that of BNIP3 or NIX. These results may indicate that high glucose triggers PINK1-dependent mitophagy in neuronal cells. Interestingly, present study found that PINK1 protein expression is increased in a dose-dependent manner although PINK1 mRNA expressions in 25 mM and 50 mM D-glucose

condition are similar. This inconsistency of PINK1 results between PCR and western blot may be responsible for PINK1 stabilization increased by high glucose-induced ROS production and mitochondrial impairment (Narendra et al., 2010b). In addition, present study results showed that high glucose stimulates co-localization of LC-3B or PINK1 with COX4 as well as stimulating expressions of LC-3B and PINK1. Those results are consistent with a recent report that platelet cells derived from DM patients have increased expression levels of LC-3 and PINK1, leading to protection against oxidative stress (Lee et al., 2016b). It has also been demonstrated that PINK1/Parkin-mediated ubiquitination of substrates including MFN, TOM, and VDAC trigger mitophagy through interaction with p62 or LC-3 even though PINK1 does not have an LC3-interacting region motif (Grenier et al., 2013; Narendra et al., 2010a; Okatsu et al., 2010; Saito and Sadoshima, 2015). Mitophagy which induces selective mitochondrial clearance has been considered as a defense mechanism against impairment of mitochondria by cellular stress that can trigger apoptosis (Kubli and Gustafsson, 2012). Previous studies have shown that high glucose leads to neuronal cell apoptosis despite the induction of PINK1-dependent mitophagy that acts as a protective factor in

neurodegeneration by preventing the apoptosis (Anichtchik et al., 2008; Lee et al., 2015; Meng et al., 2014; Moisoi et al., 2014). These findings imply that PINK1-dependent mitophagy induced by high glucose is insufficient to inhibit the neuronal cell apoptosis. Furthermore, present study results showed that PINK1 silencing enhanced cytotoxic effect of high glucose in neuronal cells via mitochondrial ROS production and dysfunction. Taken together, present study suggests the partial protective role of PINK1 against neuronal cell apoptosis under high glucose condition and PINK1-dependent mitophagy as a key regulator of mitochondrial quality control and anti-apoptosis in neuronal cells under high glucose condition. Because of PINK1's antioxidative effect, PINK1 induction has been suggested as a promising strategy for treatment of neuronal apoptosis in neurodegenerative diseases such as Parkinson's disease (Petit et al., 2005; Pridgeon et al., 2007; Valente et al., 2004; Wood-Kaczmar et al., 2008).

Although it has been reported that melatonin induces PINK1 (Diaz-Casado et al., 2016; Kang et al., 2016). the effect of melatonin on mitophagy regulators in human neuronal cells has not been described fully. In the present study confirmed a stimulatory effect of melatonin on PINK1, but not BNIP3 or NIX, in SK-N-MC cells. In addition,

present study results demonstrate that melatonin can be a significant inducer of PINK1-dependent mitophagy in neuronal cells. Melatonin's antioxidative mechanism has been well documented, but several researchers have also indicated that melatonin has a conditional ROS stimulatory potential (Zhang and Zhang, 2014). This twofold effect of melatonin seems to vary according to glucose concentration, glucose treatment duration, and cell type. In the present study results showed melatonin treatment significantly suppressed mitochondrial ROS accumulation and mitochondrial membrane potential impairment in neuronal cell under high glucose conditions. This present study results support those of Silvia Cristofanon, et al. who reported that melatonin-activated NF-κB signaling pathway is responsible for a survival (Cristofanon et al., 2009). In addition, this present study observed that high glucose stimulates MT_2 expression, and that PINK1 induction by melatonin is dependent on the MT_2 signaling pathway in SK-N-MC and SH-SY5Y cells and in mouse hippocampal neurons, a pathway that is critical for neuronal cell survival under high glucose conditions. This is the first report of MT_2 being an initiative mediator of melatonin-induced PINK1 expression in neuronal cells. Similar to the neuroprotective effect of melatonin, a previous report showed that

MT_2 expression was increased in hippocampal region astrocytes exposed to ischemic injury, indicating that MT_2 expression in neuronal cells may be associated with oxidative stress (Lee et al., 2010). This present study assumed that high glucose-induced ROS is associated with the increase of MT_2 expression in present study experimental condition. Actually, this present study data showed that NAC pretreatment reduced the increase of MT_2 receptor expression by high glucose. However, the further investigation is required to better understand the underlying mechanisms, which are involved in MT_2 expression by high glucose-induced ROS in neuroblastoma cell lines. Taken together, current and previous results suggest that neuronal cells exposed to a high glucose condition have high sensitivity to melatonin, and that sensitivity is associated with MT_2-specific physiological regulation of melatonin in DM patients. In addition, there have been several reports indicating distinct roles of melatonin receptors in the pathogenesis of neurological disorders. Indeed, previous studies have reported that increased MT_1 and MT_2 levels are associated with Alzheimer's disease and ischemic neuronal injury, respectively, and that decreased MT_1 and MT_2 levels are observed in Parkinson's disease (Adi et al., 2010; Lee et al., 2010; Savaskan et al.,

2001). However, there are no reports describing a role of MT_1 in hyperglycemia-associated neuronal cell death. Further investigation will be required to elucidate the role of melatonin receptors in melatonin-based treatment of DM patients with neurologic complications.

This present study findings suggest high glucose increased phosphorylations of Akt and NF-κB. It has been documented that increment of intracellular ROS activates PI3K/Akt signaling in the neuronal cells, which has a capacity for regulation of NF-κB activity (Bai et al., 2009; Sadidi et al., 2009). Those findings indicate that ROS is an upstream regulator of Akt/NF-κB pathway induced by high glucose treatment. Furthermore, present study investigation revealed that Akt/NF-κB signaling activated by MT_2 is important for PINK1-mediated neuronal cell survival under high glucose conditions. The C-terminal motif of activated MT_2 directly binds to Akt, which leads to regulation of neuronal cell-related physiology including hypothalamus-liver communication, axonogenesis, and synaptic transmission (Anhe et al., 2004; Liu et al., 2015). In addition, it has been reported that Akt phosphorylation by melatonin induces neuroprotective effect (Kong et al., 2008). Although several

investigators have reported that MT_2 and heteromeric MT_1/MT_2 receptors activate ERK1/2 and PKC pathways (Baba et al., 2013; Luchetti et al., 2010; Radio et al., 2006), present study observed that melatonin treatment did not affect the phosphorylation levels of ERK1/2 and pan PKC (Fig. 18C). In addition, present study results showed the MT_2 stimulates PINK1 expression via augmentation of the high glucose-activated Akt/NF-κB pathway, which indicates that incorporation of melatonin-induced MT_2 signaling into high glucose signaling is required for PINK1 expression. A previous study identified the NF-κB binding site within the transcription start site of the human PINK1 gene promoter and suggested NF-κB as a significant regulator of PINK1 expression in neuronal cells (Duan et al., 2014). These findings suggest that activation of the Akt/NF-κB pathway by melatonin is crucial in the regulation of PINK1 expression. Meanwhile, another report described nuclear factor (erythroid-derived 2)-like 2 (NRF2) as a PINK1 inducer involved in neuronal cell survival under oxidative stress (Murata et al., 2015). This observation suggests the possibility that NRF2 may also contribute to PINK1 expression in neuronal cell protection against oxidative stress under high glucose conditions. For example, it has been reported that melatonin-activated

MT_2 signaling has a regulatory role in the attenuation of memory impairment via a NRF2-associated antioxidative effect (Shin et al., 2014Shin et al., 2014). Although the present study demonstrated that MT_2-induced NF-κB is a key factor in PINK1 expression, additional research will be needed to determine the role of NRF2 in melatonin-induced PINK1 expression of neuronal cells.

In conclusion, this present study has demonstrated that melatonin enhances PINK1-dependent mitophagy via the MT_2/Akt/NF-κB pathway, and such mitophagy is critical for high glucose-induced mitochondrial impairment and apoptosis in neuronal cells (Fig. 23). This present study proposes the melatonin-induced PINK1 is a key factor in the regulation of ROS accumulation and anti-apoptosis in neuronal cells under high glucose conditions. To study knowledge, this present study investigation is the first to demonstrate a detailed mechanism controlling PINK1 expression by melatonin in neuronal cells under high glucose conditions. Identification of the pathways involved in controlling PINK1 by high glucose and melatonin will provide novel insights that will be useful in the development of therapeutic strategies for the treatment of hyperglycemia-associated neuronal cell death.

REFERENCES

Adi, N., Mash, D.C., Ali, Y., Singer, C., Shehadeh, L., and Papapetropoulos, S. (2010). Melatonin MT_1 and MT_2 receptor expression in Parkinson's disease. Med Sci Monit 16, BR61-67.

Anhe, G.F., Caperuto, L.C., Pereira-Da-Silva, M., Souza, L.C., Hirata, A.E., Velloso, L.A., Cipolla-Neto, J., and Carvalho, C.R. (2004). In vivo activation of insulin receptor tyrosine kinase by melatonin in the rat hypothalamus. J Neurochem 90, 559-566.

Anichtchik, O., Diekmann, H., Fleming, A., Roach, A., Goldsmith, P., and Rubinsztein, D.C. (2008). Loss of PINK1 function affects development and results in neurodegeneration in zebrafish. J Neurosci 28, 8199-8207.

Antolin, I., Mayo, J.C., Sainz, R.M., del Brio Mde, L., Herrera, F., Martin, V., and Rodriguez, C. (2002). Protective effect of melatonin in a chronic experimental model of Parkinson's disease. Brain Res 943, 163-173.

Baba, K., Benleulmi-Chaachoua, A., Journe, A.S., Kamal, M., Guillaume, J.L., Dussaud, S., Gbahou, F., Yettou, K., Liu, C., Contreras-Alcantara, S., Jockers, R., Tosini, G. (2013). Heteromeric MT_1/MT_2 melatonin receptors modulate photoreceptor function. Sci Signal 6, ra89.

Bai, D., Ueno, L., and Vogt, P.K. (2009). Akt-mediated regulation of NFkappaB and the essentialness of NFkappaB for the oncogenicity of PI3K and Akt. Int J Cancer 125, 2863-2870.

Bellot, G., Garcia-Medina, R., Gounon, P., Chiche, J., Roux, D., Pouyssegur, J., and Mazure, N.M. (2009). Hypoxia-induced autophagy is mediated through hypoxia-inducible factor induction of BNIP3 and BNIP3L via their BH3 domains. Mol Cell Biol 29, 2570-2581.

Bonnefond, A., and Froguel, P. (2017). The case for too little melatonin signalling in increased diabetes risk. Diabetologia 60, 823-825.

Chen, S.T., and Chuang, J.I. (1999). The antioxidant melatonin reduces cortical neuronal death after intrastriatal injection of kainate in the rat. Exp Brain Res 124, 241-247.

Costes, S., Boss, M., Thomas, A.P., and Matveyenko, A.V. (2015). Activation of Melatonin Signaling Promotes beta-Cell Survival and Function. Mol Endocrinol 29, 682-692.

Coto-Montes, A., Boga, J.A., Rosales-Corral, S., Fuentes-Broto, L., Tan, D.X., and Reiter, R.J. (2012). Role of melatonin in the regulation of autophagy and mitophagy: a review. Mol Cell Endocrinol 361, 12-23.

Cristofanon, S., Uguccioni, F., Cerella, C., Radogna, F., Dicato, M., Ghibelli, L., and Diederich, M. (2009). Intracellular prooxidant activity of melatonin induces a survival pathway involving NF-kappaB activation. Ann N Y Acad Sci 1171, 472-478.

Den Heijer, T., Vermeer, S.E., van Dijk, E.J., Prins, N.D., Koudstaal, P.J., Hofman, A., and Breteler, M.M. (2003). Type 2 diabetes and atrophy of medial temporal lobe structures on brain MRI. Diabetologia 46, 1604-1610.

Diaz-Casado, M.E., Lima, E., Garcia, J.A., Doerrier, C., Aranda, P., Sayed, R.K., Guerra-Librero, A., Escames, G., Lopez, L.C., and Acuna-Castroviejo, D. (2016). Melatonin rescues zebrafish embryos from the parkinsonian phenotype restoring the parkin/PINK1/DJ-1/MUL1 network. J Pineal Res 61, 96-107.

Duan, X., Tong, J., Xu, Q., Wu, Y., Cai, F., Li, T., and Song, W. (2014). Upregulation of human PINK1 gene expression by NFkB signalling. Mol Brain 7, 57.

Fan, F., Liu, T., Wang, X., Ren, D., Liu, H., Zhang, P., Wang, Z., Liu, N., Li, Q., Tu, Y., Yu, J. (2016). ClC-3 Expression and Its Association with Hyperglycemia Induced HT22 Hippocampal Neuronal Cell Apoptosis. J Diabetes Res 2016, 2984380.

Frank, M., Duvezin-Caubet, S., Koob, S., Occhipinti, A., Jagasia, R., Petcherski, A., Ruonala, M.O., Priault, M., Salin, B., and Reichert, A.S. (2012). Mitophagy is triggered by mild oxidative stress in a mitochondrial fission dependent manner. Biochim Biophys Acta 1823, 2297-2310.

Gandhi, S., Wood-Kaczmar, A., Yao, Z., Plun-Favreau, H., Deas, E., Klupsch, K., Downward, J., Latchman, D.S., Tabrizi, S.J., Wood, N.W., Duchen, M.R., Abramov, A.Y. (2009). PINK1-associated Parkinson's disease is caused by neuronal vulnerability to calcium-induced cell death. Mol Cell 33, 627-638.

Grenier, K., McLelland, G.L., and Fon, E.A. (2013). Parkin- and PINK1-Dependent Mitophagy in Neurons: Will the Real Pathway Please Stand Up? Front Neurol 4, 100.

Hoshino, A., Ariyoshi, M., Okawa, Y., Kaimoto, S., Uchihashi, M., Fukai, K., Iwai-Kanai, E., Ikeda, K., Ueyama, T., Ogata, T.Matoba,S (2014). Inhibition of p53 preserves Parkin-mediated mitophagy and pancreatic beta-cell function in diabetes. Proc Natl Acad Sci USA 111, 3116-3121.

Huang, C., Zhang, Y., Kelly, D.J., Tan, C.Y., Gill, A., Cheng, D., Braet, F., Park, J.S., Sue, C.M., Pollock, C.A.,Chen X.M. (2016). Thioredoxin interacting protein (TXNIP) regulates tubular autophagy and mitophagy in diabetic nephropathy through the mTOR signaling pathway. Sci Rep 6, 29196.

Jockers, R., Maurice, P., Boutin, J.A., and Delagrange, P. (2008). Melatonin receptors, heterodimerization, signal transduction and binding sites: what's new? Br J Pharmacol 154, 1182-1195.

Kang, J.W., Hong, J.M., and Lee, S.M. (2016). Melatonin enhances mitophagy and mitochondrial biogenesis in rats with carbon tetrachloride-induced liver fibrosis. J Pineal Res 60, 383-393.

Kong, P.J., Byun, J.S., Lim, S.Y., Lee, J.J., Hong, S.J., Kwon, K.J., and Kim, S.S. (2008). Melatonin Induces Akt Phosphorylation through Melatonin Receptor- and PI3K-Dependent Pathways in Primary Astrocytes. Korean J Physiol Pharmacol 12, 37-41.

Kubli, D.A., and Gustafsson, A.B. (2012). Mitochondria and mitophagy: the yin and yang of cell death control. Circ Res 111, 1208-1221.

Kumar, P., Raman, T., Swain, M.M., Mishra, R., and Pal, A. (2017). Hyperglycemia-Induced Oxidative-Nitrosative Stress Induces Inflammation and Neurodegeneration via Augmented Tuberous Sclerosis Complex-2 (TSC-2) Activation in Neuronal Cells. Mol Neurobiol 54, 238-254.

Lee, C.H., Yoo, K.Y., Choi, J.H., Park, O.K., Hwang, I.K., Kwon, Y.G., Kim, Y.M., and Won, M.H. (2010). Melatonin's protective action against ischemic neuronal damage is associated with up-regulation of the MT_2 melatonin receptor. J Neurosci Res 88, 2630-2640.

Lee, H.J., Ryu, J.M., Jung, Y.H., Lee, S.J., Kim, J.Y., Lee, S.H., Hwang, I.K., Seong, J.K., and Han, H.J. (2016a). High glucose upregulates BACE1-mediated Abeta production through ROS-dependent HIF-1alpha and LXRalpha/ABCA1-regulated lipid raft reorganization in SK-N-MC cells. Sci Rep 6, 36746.

Lee, S.H., Du, J., Stitham, J., Atteya, G., Lee, S., Xiang, Y., Wang, D., Jin, Y., Leslie, K.L., Spollett, G., Srivastava, A., Mannam, P., Ostriker, A., Martin, K.A., Tang, W.H., Hwa, J. (2016b). Inducing mitophagy in diabetic platelets protects against EMBO Mol Med 8, 779-795.

Li, Y., Xu, S., Zhang, Q., Li, L., Lai, L., Zheng, T., Su, J., Yang, N., and Li, Y. (2014). Cytotoxicity study on SHSY5Y cells cultured at high glucose levels and treated with bupivacaine. Mol Med Rep 9, 515-520.

Liu, D., Wei, N., Man, H.Y., Lu, Y., Zhu, L.Q., and Wang, J.Z. (2015). The MT_2 receptor stimulates axonogenesis and enhances synaptic transmission by activating Akt signaling. Cell Death Differ 22, 583-596.

Liu, L., Sakakibara, K., Chen, Q., and Okamoto, K. (2014). Receptor-mediated mitophagy in yeast and mammalian systems. Cell Res 24, 787-795.

Lo, M.C., Lu, C.I., Chen, M.H., Chen, C.D., Lee, H.M., and Kao, S.H. (2010). Glycoxidative stress-induced mitophagy modulates mitochondrial fates. Ann N Y Acad Sci 1201, 1-7.

Luchetti, F., Canonico, B., Betti, M., Arcangeletti, M., Pilolli, F., Piroddi, M., Canesi, L., Papa, S., and Galli, F. (2010). Melatonin signaling and cell protection function. FASEB J 24, 3603-3624.

Lyssenko, V., Nagorny, C.L., Erdos, M.R., Wierup, N., Jonsson, A., Spegel, P., Bugliani, M., Saxena, R., Fex, M., Pulizzi, N., Isomaa, B., Tuomi, T., Nilsson, P., Kuusisto, J., Tuomilehto, J., Boehnke, M., Altshuler, D., Sundler, F., Eriksson, J.G., Jackson, A.U., Laakso, M., Marchetti, P., Watanabe, R.M., Mulder, H., Groop, L. (2009). Common variant in MTNR1B associated with increased risk of type 2 diabetes and impaired early insulin secretion. Nat Genet 41, 82-88.

Manchester, L.C., Coto-Montes, A., Boga, J.A., Andersen, L.P., Zhou, Z., Galano, A., Vriend, J., Tan, D.X., and Reiter, R.J. (2015). Melatonin: an ancient molecule that makes oxygen metabolically tolerable. J Pineal Res 59, 403-419.

Mattson, M.P. (2000). Apoptosis in neurodegenerative disorders. Nat Rev Mol Cell Biol 1, 120-129.

McMullan, C.J., Schernhammer, E.S., Rimm, E.B., Hu, F.B., and Forman, J.P. (2013). Melatonin secretion and the incidence of type 2 diabetes. JAMA 309, 1388-1396.

Melser, S., Chatelain, E.H., Lavie, J., Mahfouf, W., Jose, C., Obre, E., Goorden, S., Priault, M., Elgersma, Y., Rezvani, H.R., Rossignol, R., Benard, G. (2013). Rheb regulates mitophagy induced by mitochondrial energetic status. Cell Metab 17, 719-730.

Meng, X., Wang, X., Tian, X., Yang, Z., Li, M., and Zhang, C. (2014). Protection of neurons from high glucose-induced injury by deletion of MAD2B. J Cell Mol Med 18, 844-851.

Moisoi, N., Fedele, V., Edwards, J., and Martins, L.M. (2014). Loss of PINK1 enhances neurodegeneration in a mouse model of Parkinson's disease triggered by mitochondrial stress. Neuropharmacology 77, 350-357.

Moruno, F., Perez-Jimenez, E., and Knecht, E. (2012). Regulation of autophagy by glucose in Mammalian cells. Cells 1, 372-395.

Moussavi, S., Chatterji, S., Verdes, E., Tandon, A., Patel, V., and Ustun, B. (2007). Depression, chronic diseases, and decrements in health: results from the World Health Surveys. Lancet 370, 851-858.

Murata, H., Takamatsu, H., Liu, S., Kataoka, K., Huh, N.H., and Sakaguchi, M. (2015). NRF2 Regulates PINK1 Expression under Oxidative Stress Conditions. PloS One 10, e0142438.

Narendra, D., Kane, L.A., Hauser, D.N., Fearnley, I.M., and Youle, R.J. (2010). p62/SQSTM1 is required for Parkin-induced mitochondrial clustering but not mitophagy; VDAC1 is dispensable for both. Autophagy 6, 1090-1106.

Narendra, D.P., Jin, S.M., Tanaka, A., Suen, D.F., Gautier, C.A., Shen, J., Cookson, M.R., and Youle, R.J. (2010b). PINK1 is selectively stabilized on impaired mitochondria to activate Parkin. PLoS Biol 8, e1000298.

Okatsu, K., Saisho, K., Shimanuki, M., Nakada, K., Shitara, H., Sou, Y.S., Kimura, M., Sato, S., Hattori, N., Komatsu, M.,Tanaka, K., Matsuda, N. (2010). p62/SQSTM1 cooperates with Parkin for perinuclear clustering of depolarized mitochondria. Genes Cells 15, 887-900.

Petit, A., Kawarai, T., Paitel, E., Sanjo, N., Maj, M., Scheid, M., Chen, F., Gu, Y., Hasegawa, H., Salehi-Rad, S., Wang, L., Rogaeva, E., Fraser, P., Robibson, B., St George-Hyslop, P., Tandon, A. (2005). Wild-type PINK1 prevents basal and induced neuronal apoptosis, a protective effect abrogated by Parkinson disease-related mutations. J Biol Chem 280, 34025-34032.

Pridgeon, J.W., Olzmann, J.A., Chin, L.S., and Li, L. (2007). PINK1 protects against oxidative stress by phosphorylating mitochondrial chaperone TRAP1. PLoS Biol 5, e172.

Radio, N.M., Doctor, J.S., and Witt-Enderby, P.A. (2006). Melatonin enhances alkaline phosphatase activity in differentiating human adult mesenchymal stem cells grown in osteogenic medium via MT_2 melatonin receptors and the MEK/ERK (1/2) signaling cascade. J Pineal Res 40, 332-342.

Reiter, R.J., Tan, D.X., Mayo, J.C., Sainz, R.M., Leon, J., and Czarnocki, Z. (2003). Melatonin as an antioxidant: biochemical mechanisms and pathophysiological implications in humans. Acta Biochim Pol 50, 1129-1146.

Sadidi, M., Lentz, S.I., and Feldman, E.L. (2009). Hydrogen peroxide-induced Akt phosphorylation regulates Bax activation. Biochimie 91, 577-585.

Saito, T., and Sadoshima, J. (2015). Molecular mechanisms of mitochondrial autophagy/mitophagy in the heart. Circ Res 116, 1477-1490.

Saravia, F.E., Beauquis, J., Revsin, Y., Homo-Delarche, F., de Kloet, E.R., and De Nicola, A.F. (2006). Hippocampal neuropathology of diabetes mellitus is relieved by estrogen treatment. Cell Mol Neurobiol 26, 943-957.

Savaskan, E., Olivieri, G., Brydon, L., Jockers, R., Krauchi, K., Wirz-Justice, A., and Muller-Spahn, F. (2001). Cerebrovascular melatonin MT_1-receptor alterations in patients with Alzheimer's disease. Neurosci Lett 308, 9-12.

Scheele, C., Nielsen, A.R., Walden, T.B., Sewell, D.A., Fischer, C.P., Brogan, R.J., Petrovic, N., Larsson, O., Tesch, P.A., Wennmalm, K., Hutchinson, D.S., Cannon, B., Wahletedt, C., Pedersen, B.K., Timmons, J.A. (2007). Altered regulation of the PINK1 locus: a link between type 2 diabetes and neurodegeneration? FASEB J 21, 3653-3665.

Shin, E.J., Chung, Y.H., Le, H.L., Jeong, J.H., Dang, D.K., Nam, Y., Wie, M.B., Nah, S.Y., Nabeshima, Y., Nabeshima, T., Kim, H.C. (2014). Melatonin attenuates memory impairment induced by Klotho gene deficiency via interactive signaling between MT_2 receptor, ERK, and Nrf2-related antioxidant potential. Int J Neuropsychopharmacol 18.

Sima, A.A. (2010). Encephalopathies: the emerging diabetic complications. Acta Diabetol 47, 279-293.

Soleimanpour, S.A., Gupta, A., Bakay, M., Ferrari, A.M., Groff, D.N., Fadista, J., Spruce, L.A., Kushner, J.A., Groop, L., Seeholzer, S.H., Kaufman, B.A., Hakonarson, H., Stoffers, D.A. (2014). The diabetes susceptibility gene Clec16a regulates mitophagy. Cell 157, 1577-1590.

Staiger, H., Machicao, F., Schafer, S.A., Kirchhoff, K., Kantartzis, K., Guthoff, M., Silbernagel, G., Stefan, N., Haring, H.U., and Fritsche, A. (2008). Polymorphisms within the novel type 2 diabetes risk locus MTNR1B determine beta-cell function. PloS One 3, e3962.

Stovring, H., Harmsen, C.G., Wisloff, T., Jarbol, D.E., Nexoe, J., Nielsen, J.B., and Kristiansen, I.S. (2013). A competing risk approach for the European Heart SCORE model based on cause-specific and all-cause mortality. Eur J Prev Cardiol 20, 827-836.

Suzuki, M., Sasabe, J., Furuya, S., Mita, M., Hamase, K., and Aiso, S. (2012). Type 1 diabetes mellitus in mice increases hippocampal D-serine in the acute phase after streptozotocin injection. Brain Res 1466, 167-176.

Tang, Y., Liu, J., and Long, J. (2015). Phosphatase and tensin homolog-induced putative kinase 1 and Parkin in diabetic heart: Role of mitophagy. J Diabetes Investig 6, 250-255.

Tuomi, T., Nagorny, C.L., Singh, P., Bennet, H., Yu, Q., Alenkvist, I., Isomaa, B., Ostman, B., Soderstrom, J., Pesonen, A.K., Martikainen, S., Räikkönen, K., Forsén, T., Hakaste, L., Almgren, P., Storm, P., Asplund, O., Shcherbina, L., Fex, M., Fadista, J., Tengholm, A., Wierup, N., Groop, L., Mulder, H. (2016). Increased Melatonin Signaling Is a Risk Factor for Type 2 Diabetes. Cell Metab 23, 1067-1077.

Valente, E.M., Abou-Sleiman, P.M., Caputo, V., Muqit, M.M., Harvey, K., Gispert, S., Ali, Z., Del Turco, D., Bentivoglio, A.R., Healy, D.G., Albanese, A., Nussbaum, R., Gonzalez-Maldonado, R., Deller, T., Salvi, S., Cortelli, P., Gilks, W.P., Latchman, D.s., Harvey, R.J., Auburger, G., Wood, N.W. (2004). Hereditary early-onset Parkinson's disease caused by mutations in PINK1. Science 304, 1158-1160.

Vikram, A., Tripathi, D.N., Kumar, A., and Singh, S. (2014). Oxidative stress and inflammation in diabetic complications. Int J Endocrinol 2014, 679754.

Wang, P., Sun, X., Wang, N., Tan, D.X., and Ma, F. (2015a). Melatonin enhances the occurrence of autophagy induced by oxidative stress in Arabidopsis seedlings. J Pineal Res 58, 479-489.

Wang, X., Yu, S., Wang, C.Y., Wang, Y., Liu, H.X., Cui, Y., and Zhang, L.D. (2015b). Advanced glycation end products induce oxidative stress and mitochondrial dysfunction in SH-SY5Y cells. In Vitro Cell Dev Biol Anim 51, 204-209.

Wood-Kaczmar, A., Gandhi, S., Yao, Z., Abramov, A.Y., Miljan, E.A., Keen, G., Stanyer, L., Hargreaves, I., Klupsch, K., Deas, E., Downward, J., Mansfield, L., Jat, P., Taylor, J., Heales, S., Duchen, M.R., Latchman, D., Tabrizi, S.J., Wood, N.W. (2008). PINK1 is necessary for long term survival and mitochondrial function in human dopaminergic neurons. PLoS One 3, e2455.

Zhang, H.M., and Zhang, Y. (2014). Melatonin: a well-documented antioxidant with conditional pro-oxidant actions. J Pineal Res 57, 131-146.

Zhou, W., Yang, J., Zhang, D.I., Li, F., Li, G., Gu, Y., and Luo, M. (2015). Role of Bcl-2/adenovirus E1B 19 kDa-interacting protein 3 in myocardial cells in diabetes. Exp Ther Med 10, 67-73.

국 문 초 록

고포도당에 의한 신경세포 자멸사에 멜라토닌 매개 MT2/Akt/NF-kB 신호전달 경로를 통한 PINK1 발현이 미치는 영향

서울대학교 대학원

수의학과 수의생명과학 전공

사이캄 언파잔

지도교수 한 호 재

고혈당증은 당뇨병의 대표적인 위험인자로서 당뇨병 매개 신경세포사멸과 밀접하게 연관되어 있다. 이전의 연구자들은 광범위 유전체연구를 통해서 당뇨병에서 멜라토닌 수용체 신호전달경로의 역할을 규명함으로써 당뇨병과 멜라토닌 수용체간의 상관관계를 보여주었다. 하지만, 당뇨병의 발병기전에 있어서 멜라토닌 수용체의 역할은 명확하지 않다. 따라서, 이번 연구는 고포도당 유도 신경세포 사멸에 있어서 미토콘드리아

자가섭식작용 조절자의 역할과 멜라토닌이 이에 미치는 영향을 밝히기 수행되었으며, 연구결과는 아래와 같다. 신경세포모델에서 고포도당 처리는 PINK1과 LC-3B 발현을 증가시켰으며, COX4 발현과 미토콘드리아 표지자의 발현을 감소시켰다. siRNA를 이용한 PINK1 발현 억제 실험에서 미토콘드리아 내 활성산소종 생성 증가와 미토콘드리아 막전위 감소가 확인되었으며, 활성형 캐스파아제 발현과 아넥신 V 양성 세포수는 증가되었다. 고포도당 환경에 노출된 신경세포는 PINK1발현과 2형 멜라토닌 수용체의 발현이 증가되었으며, 활성산소종 차단제 전처리에 의해서 PINK1과 2형 멜라토닌 수용체의 발현이 감소되었다. 멜라토닌처리는 고포도당 환경에 의해 유도된 PINK1 발현을 항진시켰으며, 이는 2형 멜라토닌 수용체 억제제 전처리에 의해서 감소되었다. 멜라토닌 처리에 의한 Akt/NF-κB 인산화는 NF-κB의 핵 내 이동 유도를 통하여 PINK1의 발현을 증가시켰다. 또한, PINK1 발현의 억제는 멜라토닌 처리를 통해 감소되었던 활성산소종 생성과 활성형 캐스파아제 발현, 아넥신 V 양성세포수를 증가시켰다. 결론적으로, 멜라토닌은 신경세포에서 MT_2/Akt/NF-κB 신호전달경로를 통해서 PINK1 발현을 촉진시키며, 고포도당상태에서의 신경세포 자멸사를 억제시켰다.

주요어: 당뇨병, 포도당, 멜라토닌, PINK1, 신경세포 자멸사

학번: 2015-22386